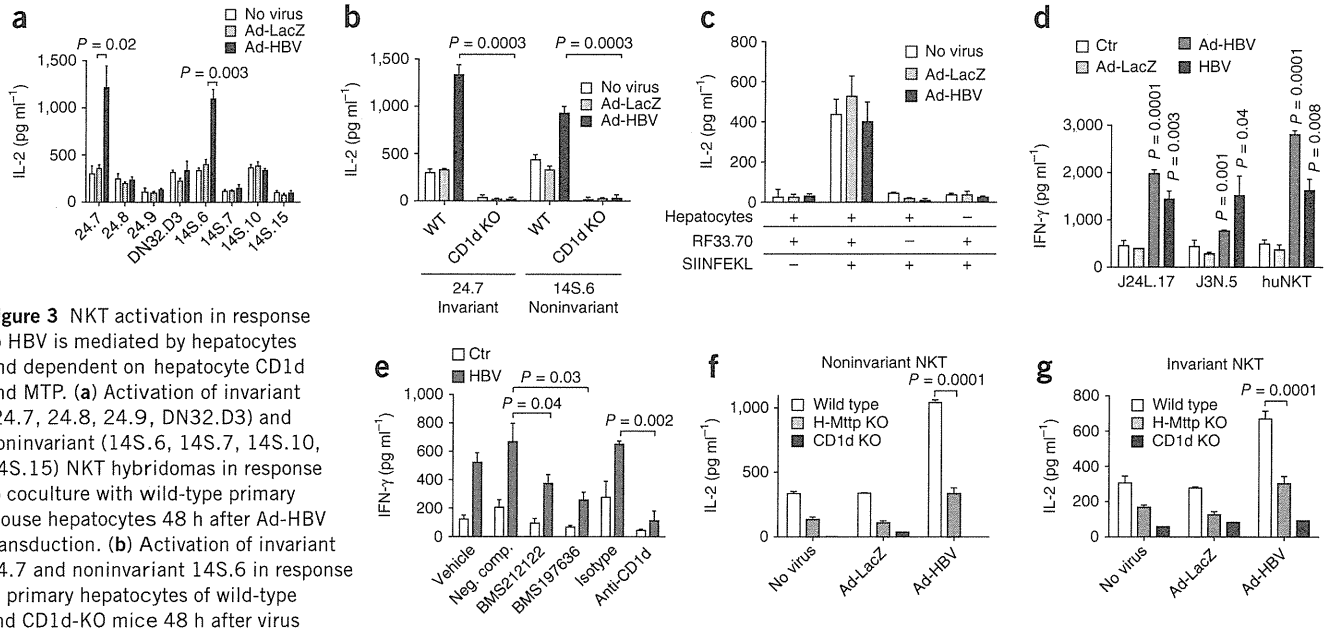

Figure 3 NKT activation in response to HBV is mediated by hepatocytes and dependent on hepatocyte CD1d and MTP. (**a**) Activation of invariant (24.7, 24.8, 24.9, DN32.D3) and noninvariant (14S.6, 14S.7, 14S.10, 14S.15) NKT hybridomas in response to coculture with wild-type primary mouse hepatocytes 48 h after Ad-HBV transduction. (**b**) Activation of invariant 24.7 and noninvariant 14S.6 in response to primary hepatocytes of wild-type and CD1d-KO mice 48 h after virus administration. Viral transduction was similar in hepatocytes from both strains (see **Supplementary Fig. 9**). (**c**) Activation of the MHC class I–restricted T cell hybridoma RF33.70 in response to SIINFEKL (1 μg ml^{-1}) presented by primary hepatocytes 48 h post infection. (**d**) Activation of human iNKT cell clones J24L.17 and J3N.5 and Jα24Vβ11-positive human iNKT cells (huNKT) expanded from peripheral blood in response to human hepatocytes infected with Ad-LacZ, Ad-HBV, or a primary HBV isolate. (**e**) IFN-γ secretion by J24L.17 NKT cells, as determined 72 h after HBV infection of primary human hepatocytes and 48 h after treatment with CD1d-blocking antibodies and MTP inhibitors (BMS212122, BMS197636) or a structurally related negative compound. (**f**,**g**) Activation of noninvariant 14S.6 (**f**) and invariant 24.7 (**g**) by primary hepatocytes from the indicated mouse strains 48 h after infection with the indicated viruses or vehicle. Cytokine secretion in **a**–**g** was determined by ELISA 24 h after coculture. Mean ± s.e.m. of triplicate cultures are shown. Results are representative of three independent experiments.

Similarly, iNKT cell activation by hepatocytes loaded with the exogenous model lipid α-galactosylceramide (αGalCer) was not affected by Ad-HBV (**Supplementary Fig. 12c**). Given that nucleocapsid-free subviral HBsAg particles, which are produced at considerably higher numbers compared to complete HBV virions[27], bud at ER and Golgi membranes[28] and selectively recruit ER lipids for their envelopes[29], we investigated whether HBV-induced NKT activation is the consequence of alterations in endogenous ER-acquired CD1d lipids. We studied activation of NKT hybridomas in response to plate-bound CD1d loaded with lipids obtained from Ad-HBV–infected primary mouse hepatocytes. We found that even uninfected primary hepatocytes contained antigenic CD1d lipids that were enriched in microsomal ER preparations (**Supplementary Fig. 13a–e**). However, microsomes from Ad-HBV– but not Ad-LacZ–transduced hepatocytes showed significantly increased activation of invariant and noninvariant NKT cell hybridomas (**Fig. 4a,b**) compared to microsomes from uninfected hepatocytes. Microsomal lipids obtained from CD1d-deficient and H-*Mttp*$^{-/-}$ hepatocytes showed similar NKT cell activation (**Supplementary Fig. 13f** and data not shown), indicating that antigenic lipids were unable to be loaded onto (H-*Mttp*$^{-/-}$) or presented by (CD1d-deficient mice) CD1d. Accordingly, purified MTP enhanced presentation of immunogenic Ad-HBV–dependent lipids (**Fig. 4c**).

Only a subset of NKT cell hybridomas recognized Ad-HBV–infected hepatocytes (**Fig. 3a**). Given that the TCRαβ repertoire of these hybridomas is unlikely to reflect that of liver NKT cells *in vivo*[30], we investigated the response of primary liver-derived NKT cells to hepatocyte microsomal lipids. A significant population of sorted noninvariant liver NKT cells recognized Ad-HBV–induced alterations in microsomal lipids, as determined by upregulation of CD69 expression (**Fig. 4d,e**). CD69 upregulation was less pronounced for sorted iNKT cells, suggesting that iNKT cell responses to Ad-HBV are either restricted to a subpopulation of these cells or that iNKT cells are broadly but less strongly activated by Ad-HBV (**Fig. 4d,e**). In conclusion, exposure to Ad-HBV is associated with increased antigenicity of ER lipids, which are recognized by NKT cells.

Ad-HBV induces antigenic lysophosphatidylethanolamine

To characterize Ad-HBV–dependent lipid alterations, we separated microsomal lipids obtained from hepatocytes according to solubility[31]. Ad-HBV–induced stimulatory fractions for noninvariant and invariant NKT cells were both recovered in phospholipid-enriched methanol eluents, but subfractionation indicated that the two NKT cell subtypes were activated by different lipids (**Fig. 4f,g**). To characterize the particular lipids induced by Ad-HBV and stimulatory for NKT cells, we screened methanol fractions by HPLC mass spectrometry (HPLC-MS). Previous reports demonstrated selective recruitment of ER lipids by HBV subviral particles and underrepresentation of phosphatidylethanolamine (PE) species in the HBV envelope[29]. Comparison of chromatograms corresponding to the mass and collisional spectra of diacyl PE showed strong enrichment of PE and lysophosphatidylethanolamine (lysoPE) after Ad-HBV exposure (**Supplementary Fig. 14**). Lysophospholipids have recently been shown to be antigenic endogenous CD1d ligands in human cells *in vitro*[32,33]. Therefore, we rescreened stimulatory fractions at masses corresponding to monoacyl PE species with C16, C18:2, C18:1 and C18 monacyl forms and found in all cases that these lipids were upregulated after Ad-HBV administration *in vivo* (**Fig. 5a**). Thus, there is an overlap among the types of lipids upregulated in response to Ad-HBV and lysophosopholipids that can stimulate NKT cells.

To further test initial conclusions derived from complex cellular lipid mixtures generated *in vivo*, we tested activation of mouse NKT

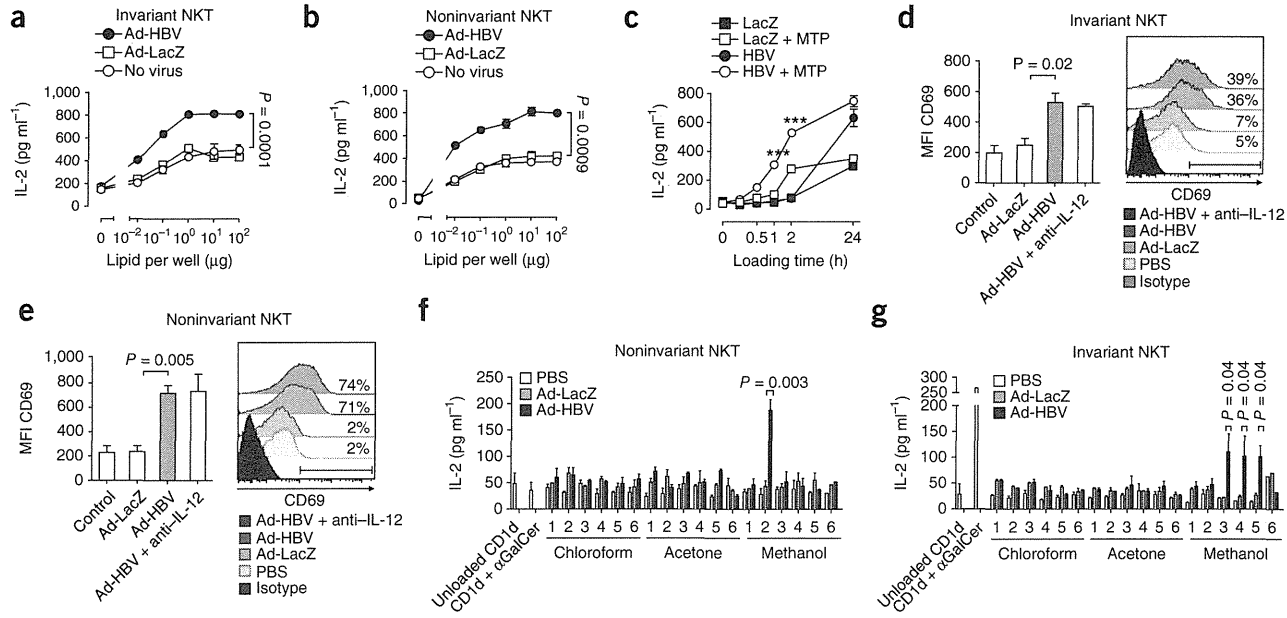

Figure 4 Microsomal lipids of Ad-HBV-infected hepatocytes contain NKT cell-activating lipid antigens. (**a–c**) IL-2 release of invariant 24.7 (**a**) and noninvariant 14S.6 (**b**) NKT cells in response to platebound CD1d loaded with microsomal lipids of hepatocytes infected with Ad-LacZ and Ad-HBV. In **c**, microsomal lipids were loaded in the presence or absence of purified MTP. ***$P = 0.0001$ of HBV versus HBV + MTP. (**d,e**) Activation of primary invariant (**d**) and noninvariant (**e**) NKT cells in response to plate-bound CD1d presenting microsomal lipids obtained from hepatocytes transduced with the indicated viruses. Invariant and noninvariant NKT cells were as sorted GFP$^+$ αGalCer–CD1d-tetramer$^+$ 4Get (**d**) and GFP$^+$ 4Get × Jα18 KO liver mononuclear cells (**e**), respectively. Flow cytometric analysis of CD69 (MFI, left; histogram, right) gated on GFP$^+$CD3$^+$ cells is shown. Numbers in histograms indicate the percentage of cells that shift in expression of CD69 compared to microsomal lipids of uninfected cells (PBS). IL-12 neutralization demonstrates absence of indirect cytokine-mediated NKT cell activation as expected in an antigen-presenting cell–free assay. (**f,g**) Activation of noninvariant 14S.6 (**f**) and invariant 24.7 (**g**) NKT cells in response to plate-bound CD1d presenting chloroform-, acetone- or methanol-soluble lipids obtained 2 d after infection with Ad-LacZ and Ad-HBV. IL-2 secretion was determined by ELISA. Mean ± s.e.m. of triplicate cultures is shown. Results are representative of two (**d,e**) or three (**a–c,f,g**) independent experiments.

hybridomas in response to various purified phospholipids *in vitro*. 14S.6, a noninvariant NKT cell hybridoma that responded to Ad-HBV (**Fig. 3a**), showed activation in response to lysoPE and lysophosphatidylcholine (lysoPC) species containing hydrocarbon chains with lengths of 16 and 18 carbons (**Fig. 5b**). As hepatocyte lysoPE but not lysoPC abundance was increased in response to Ad-HBV (**Supplementary Fig. 14**), only lysoPE is implicated in the response to Ad-HBV. NKT cell activation by lysoPE was, among hybridomas, specific for 14S.6 and not observed with other iNKT hybridomas (24.7, 24.8, 24.9 or DN32.D3) or noninvariant NKT hybridomas (14S.7, 14S.10 or 14S.15; **Fig. 5b** and data not shown). Lyso-PE–induced NKT activation required plate-bound CD1d (data not shown), and purified MTP facilitated lysoPE presentation (**Fig. 5c**). These results extended to primary NKT cells, as >50% of sorted noninvariant liver NKT cells obtained from IL-4–IRES-GFP–enhanced transcript (4Get) × Jα18-deficient mice liver NKT cells showed upregulation of CD69 expression in response to lysoPE but not PE (**Fig. 5d**). Noninvariant NKT cell activation was not limited to cells expressing Vβ14, the TCRβ chain shared by the noninvariant NKT hybridoma (14S.6) that recognized lysoPE (**Fig. 5d**). This suggests that lysoPE broadly activates noninvariant NKT cells in the liver and further reiterates the limited overlap between currently available NKT hybridomas and primary NKT cells *in vivo*. In contrast, iNKT cells did not show activation in response to lysoPE (**Fig. 5d**).

NKT cell activation is dependent on secretory phospholipases

Secretory phospholipase A_2 ($sPLA_2$) enzymes contribute to the generation of lysophospholipids recognized by NKT cells and are active within secretory compartments[33,34]. We therefore investigated the role of $sPLA_2$ in Ad-HBV–dependent NKT cell activation. Chemical inhibitors of $sPLA_2$ but not cytoplasmic PLA_2 ($cPLA_2$) prevented HBV-dependent activation of noninvariant NKT cells without affecting MHC class I presentation (**Fig. 5e** and **Supplementary Fig. 15a–g**). $sPLA_2$ inhibitors also did not affect iNKT cells, in accordance with the lack of lysoPE-dependent iNKT activation (**Fig. 5f**).

As Ad-HBV–transduction of hepatocytes leads to increased abundance of PE (**Supplementary Fig. 14b**), the substrate for PLA_2-mediated production of lysoPE, we investigated hepatocyte gene expression of $sPLA_2$ (gene names listed in **Fig. 5g**), $cPLA_2$ (*Pla2g4a*) and calcium-independent PLA_2 ($iPLA_2$, *Pla2g6a*) enzymes. Ad-HBV led to rapid and selective upregulation of $sPLA_2$ enzymes *Pla2g2c* and *Pla2g5* but not other $sPLA_2$, $cPLA_2$ and $iPLA_2$ enzymes *in vivo* (**Fig. 5g** and **Supplementary Fig. 16a**). These results are in accordance with increased hepatic PLA_2 group II and V expression in patients with viral hepatitis[35,36]. Primary mouse hepatocytes also showed Ad-HBV–induced *Pla2g2c* upregulation, confirming hepatocyte-specific effects and demonstrating that $sPLA_2$ regulation is not secondary to hepatic inflammation but a direct consequence of exposure to Ad-HBV (**Supplementary Fig. 16b**). Primary human hepatocytes exposed to Ad-HBV or a primary HBV isolate also showed upregulation of $sPLA_2$, specifically of *PLA2G2A* (**Fig. 5h**). As lysoPE activates transcription of *PLA2G2A*[37], it most likely supports its own production through a positive-feedback loop involving $sPLA_2$. Thus, HBV leads to upregulation of $sPLA_2$ group II in mouse and human hepatocytes. Specific subgroups of $sPLA_2$ differ between humans and mice

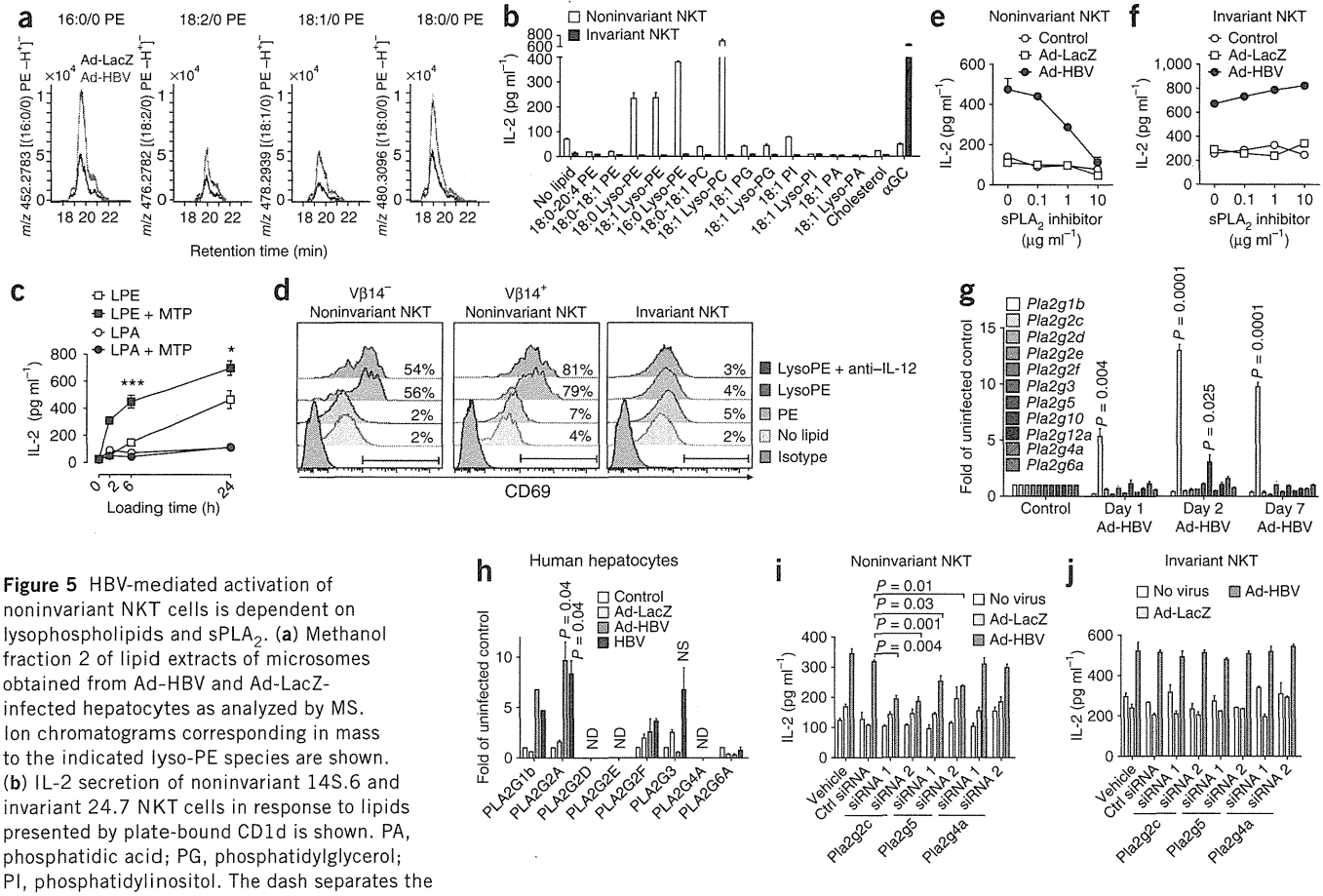

Figure 5 HBV-mediated activation of noninvariant NKT cells is dependent on lysophospholipids and $sPLA_2$. (**a**) Methanol fraction 2 of lipid extracts of microsomes obtained from Ad-HBV and Ad-LacZ-infected hepatocytes as analyzed by MS. Ion chromatograms corresponding in mass to the indicated lyso-PE species are shown. (**b**) IL-2 secretion of noninvariant 14S.6 and invariant 24.7 NKT cells in response to lipids presented by plate-bound CD1d is shown. PA, phosphatidic acid; PG, phosphatidylglycerol; PI, phosphatidylinositol. The dash separates the carbon chain length for both carbon chains in case of diacylated lipids. (**c**) IL-2 secretion by the 14S.6 noninvariant NKT cell hybridoma in response to lysophosphatidylethanolamine (LPE) and lysophosphatidic acid (LPA) presented by plate-bound CD1d and loaded in the presence or absence of purified MTP. $***P = 0.005$, $*P = 0.04$ of LPE versus LPE + MTP. (**d**) Activation of primary noninvariant (left, middle) and iNKT (right) cells in response to plate-bound CD1d presenting the indicated lipids. NKT cells were obtained as sorted invariant GFP^+ αGalCer–CD1d-tetramer$^+$ 4Get (right) and noninvariant GFP^+ 4Get × Jα18-KO liver NKT cells (left, middle). Flow cytometric analysis of CD69 gated on GFP^+ $CD3^+$ cells is shown. (**e**,**f**) Invariant 24.7 and noninvariant 14S.6 NKT cell responses to primary hepatocytes infected as indicated and treated with the $sPLA_2$ inhibitor c(2NapA)LS(2NapA)R before addition of NKT cells. (**g**) Expression of PLA_2 transcripts in mouse liver tissue after *in vivo* exposure to Ad-HBV. (**h**) Analysis of PLA_2 RNA expression in primary human hepatocytes 24 h after *in vitro* infection. Mean ± s.e.m. of triplicate cultures are shown. ND, not detectable. (**i**,**j**) IL-2 release by NKT cells in response to primary hepatocytes infected with the indicated viruses before transfection with siRNAs as indicated and coculture with NKT cells. Results are representative of two (**a**,**d**) or three (**b**,**c**,**e**–**j**) independent experiments. All data are expressed as means ± s.e.m.

in accordance with differences in the genomic organization of $sPLA_2$ loci (*PLA2G2C* is a pseudogene in humans[38]; *Pla2g2a* is inactivated by a frameshift in C57BL/6J mice).

Consistent with a crucial role for $sPLA_2$ in HBV-dependent generation of lysophospholipids as major antigens recognized by noninvariant NKT cells, siRNA directed against *Pla2g2c* and *Pla2g5* (**Supplementary Fig. 17a**) but not the genes encoding other $sPLA_2$, $cPLA_2$ and $iPLA_2$ enzymes prevented Ad-HBV–induced activation of noninvariant NKT but not invariant NKT cells or MHC class I–restricted T cells (**Fig. 5i,j** and **Supplementary Fig. 17b** and data not shown).

HBsAg contributes to NKT cell activation

To investigate the requisite HBV element for NKT cell activation, we inactivated individual HBV open reading frames and studied the effects on NKT activation. Although all viral mutants showed similar transduction rates (**Supplementary Figs. 5** and **9**), only deletion of the small HBsAg (HBsAg S^-), which is required for viral secretion, led to impaired activation of noninvariant NKT cells (**Fig. 6a**). We observed a similar but nonsignificant trend for iNKT cells (**Fig. 6b**). Ad-HBV S^- led to impaired hepatocyte $sPLA_2$ upregulation and impaired activation of noninvariant NKT cells by microsomal hepatocyte lipids (**Fig. 6c** and **Supplementary Fig. 16c**).

To extend these findings, we examined mice transgenically expressing HBsAg[19]. HBsAg-transgenic mouse hepatocytes led to CD1d-dependent activation of noninvariant and invariant NKT cell hybridomas but not MHC class I–restricted T cell hybridomas (**Fig. 6d–f**). In addition, microsomal lipids of HBsAg-transgenic hepatocytes activated NKT cells (**Fig. 6g,h**). *In vivo* administration of Ad-HBV S^- resulted in prolonged chronic necroinflammation and delayed viral control in association with sustained viral replication and impaired hepatic IFN-γ induction (**Supplementary Fig. 18**). These studies show that the small HBsAg contributes to Ad-HBV–mediated activation of NKT cells, which is in accordance with a temporal association between HBsAg expression and early NKT cell activation in human HBV infection[10].

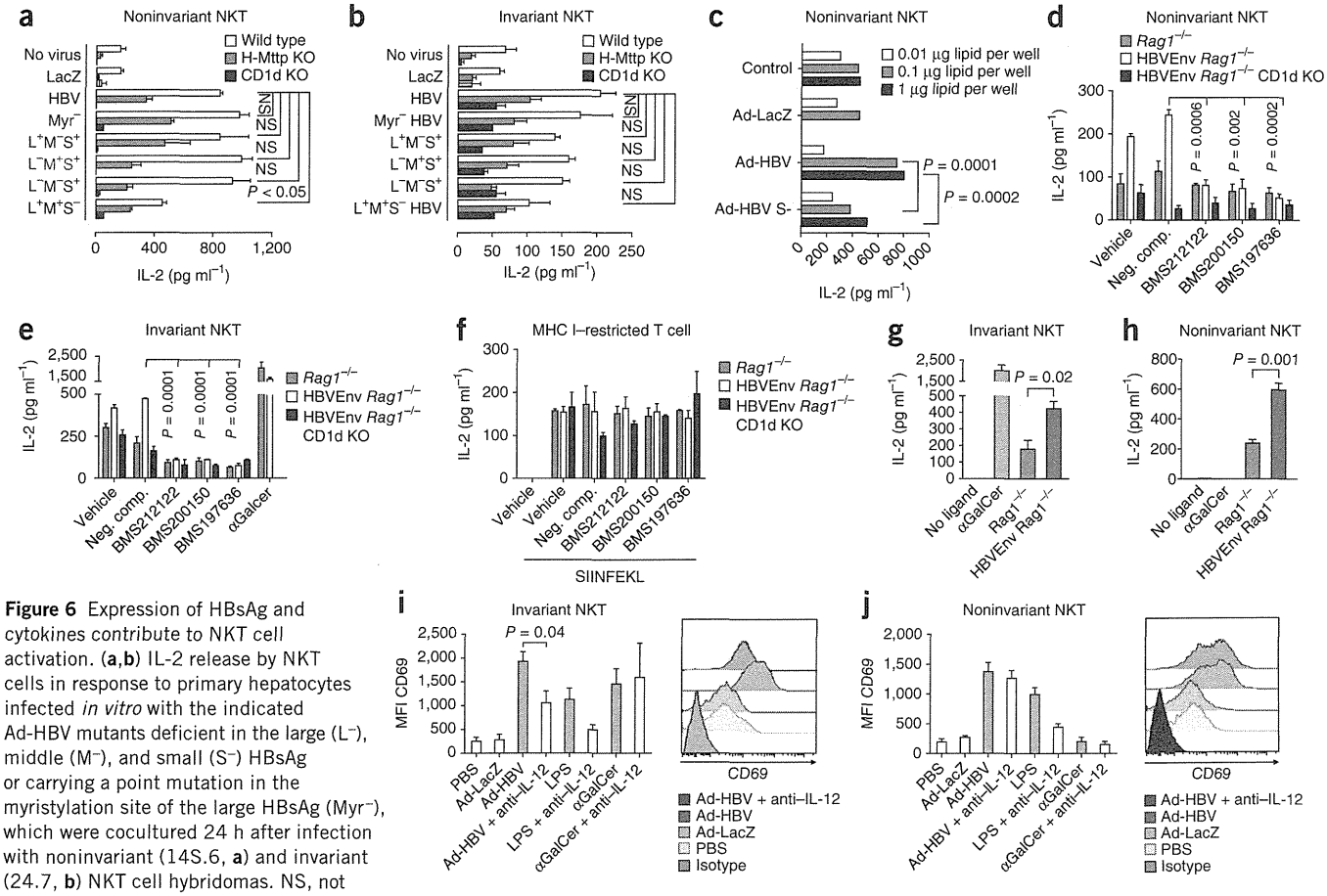

Figure 6 Expression of HBsAg and cytokines contribute to NKT cell activation. (**a**,**b**) IL-2 release by NKT cells in response to primary hepatocytes infected *in vitro* with the indicated Ad-HBV mutants deficient in the large (L^-), middle (M^-), and small (S^-) HBsAg or carrying a point mutation in the myristylation site of the large HBsAg (Myr^-), which were cocultured 24 h after infection with noninvariant (14S.6, **a**) and invariant (24.7, **b**) NKT cell hybridomas. NS, not statistically significant. (**c**) NKT cell IL-2 release in response to microsomal lipids of primary hepatocytes obtained 48 h after infection with the indicated viruses and presented by plate-bound CD1d to the noninvariant NKT cell hybridoma 14S.6. (**d**–**f**) NKT cell IL-2 release in response to primary hepatocytes of the indicated mouse strains treated with MTP inhibitors or 9-fluorenyl carboxylic acid as a negative control compound for 48 h. Hepatocytes were cocultured with noninvariant 14S.6 NKT cells (**d**), invariant 24.7 NKT cells (**e**) or MHC class I–restricted RF33.70 T cells (**f**). (**g**,**h**) NKT cell IL-2 release in response to microsomal lipids of the indicated mouse strains loaded onto plate-bound CD1d. Presentation to invariant 24.7 (**g**) and noninvariant 14S.6 (**h**) is shown. IL-2 secretion by T cell hybridomas in **a**–**h** was determined by ELISA. (**i**,**j**) Expression of CD69 as determined by flow cytometric analysis of GFP^+ αGalCer–CD1d-tetramer$^+$ $CD3^+$ invariant NKT cells (**i**) and GFP^+ αGalCer–CD1d-tetramer$^-$ $CD3^+$ noninvariant NKT cells obtained from 4Get mice injected with the indicated viruses, LPS (indirect NKT cell activation) or αGalCer (direct iNKT cell activation) in the presence or absence of antibody-mediated IL-12 neutralization. Liver mononuclear cells were obtained 6 h (αGalCer) and 24 h (viruses, LPS) after stimulation. (**j**). Representative histograms and dot plots are shown. Bar graphs show mean ± s.e.m. Results are representative of two (**d**–**j**) or three (**a**–**c**) independent experiments.

iNKT cell activation *in vivo* is cytokine dependent

Primary liver iNKT cells were not activated by lysoPE (**Fig. 5d**) and showed less robust activation in response to Ad-HBV microsomal lipids (**Fig. 4d**). We therefore investigated whether cytokine-mediated indirect activation contributes to Ad-HBV–induced iNKT cell activation *in vivo*. Indeed, neutralization of interleukin-12 (IL-12), a cytokine essential for indirect NKT cell activation[39–41], largely prevented CD69 upregulation and IFN-γ secretion by iNKT cells but had negligible effects on noninvariant NKT cells (**Fig. 6i,j** and **Supplementary Fig. 19**). These results suggest that noninvariant NKT cells are directly activated upon Ad-HBV exposure by CD1d-restricted presentation of lysoPE and other uncharacterized hepatocyte antigens. This, in turn, may lead to cytokine-dependent activation of iNKT cells, presumably through activation of liver dendritic cells and macrophages[39,40]. Notably, IL-12–mediated indirect activation of liver iNKT cells requires hepatocyte MTP (**Fig. 1a–c**), suggesting that cytokine-dependent iNKT activation is downstream of CD1d-restricted activation of noninvariant NKT cells and NKT-dependent dendritic cell maturation[42,43].

DISCUSSION

The findings presented here show that immune responses provided by NKT cells contribute not only to HBV-induced hepatitis[19] but also to viral control. Although HBV-induced NKT cell activation is associated with acute hepatitis, NKT cells contribute considerably to the emergence of antiviral B and T cell immunity. In the absence of this NKT cell response, adaptive immunity and viral control are diminished and chronic, low-grade hepatitis ensues. We show that the cell type responsible for orchestrating these HBV-induced responses is previously unappreciated and, notably, the infected hepatocyte itself and not a professional antigen-presenting cell. Within the hepatocyte, HBV induces the production of ER lipids, including lysophospholipids derived from PE through the action of HBV-induced secretory phospholipases. CD1d-restricted presentation of lysophospholipids leads to direct activation of noninvariant NKT cells and subsequent IL-12–mediated indirect iNKT cell activation, confirming that both direct and indirect mechanisms contribute to NKT cell activation *in vivo*[39,40].

The generation of antigenic lipids is partially dependent on the presence of the HBV surface antigen, the principal HBV structural

component responsible for assembling PC-rich particles in the ER, and possibly results from an imbalanced lipid milieu within the ER[29]. As such, the hepatocyte uses secretory phospholipases, MTP and CD1d to sense the presence of HBV and alert NKT cells through the display of modified self-lipids on the cell surface of the hepatocyte to trigger an adaptive immune response.

Our findings of an NKT cell response soon after HBV exposure are in accordance with other recent observations in humans and animal models of HBV[10–12] and suggest that NKT cells are part of an early, important sensing system that activates the immune response, leading to effective priming of HBV-specific adaptive immune cells that are required for viral clearance. Our data suggest that although HBV acts as a stealth virus during a prolonged phase preceding viral control[9], it is susceptible to a distinct type of immune recognition directly following infection, which is important for subsequent immune clearance. Further studies in HBV-infected humans are required to confirm a central role of NKT cells in human HBV infection.

METHODS

Methods and any associated references are available in the online version of the paper.

Note: Supplementary information is available in the online version of the paper.

ACKNOWLEDGMENTS

This work was supported by US National Institutes of Health (NIH) grants DK51362, DK44319, DK53056, DK88199, the Harvard Digestive Diseases Center DK034854 (to R.S.B.); the Deutsche Forschungsgemeinschaft (Ze 814/1-1, Ze 814/4-1), a Marie Curie International Reintegration Grant within the 7th European Community Framework Programme (256363) and the Crohn's and Colitis Foundation of America (to S.Z.); the Crohn's and Colitis Foundation of America, Austrian Science Fund, and Max Kade Foundation (to A.K.); NIH AR048632, AI049313 and the Burroughs Wellcome Fund for Translational Research (to D.B.M.); DK46900 (to M.M.H.); the NIH Intramural Research Program (K.M., Z.H. and T.J.L.); NIH grants AI068090, DK026743 and the Burroughs Wellcome Fund (to J.L.B.); and the A.P. Gianinni Foundation (to J.P.). We thank D.E. Cohen, E. Scapa and S.K. Dougan for insightful discussions.

AUTHOR CONTRIBUTIONS

S.Z. designed, performed and analyzed experiments and prepared the manuscript with R.S.B. and T.J.L.; K.M. and Z.H. generated adenoviruses and adenoviral mutants and contributed to Ad-HBV studies; L.S. and D.B.M. designed, performed and analyzed LC-MS experiments together with S.Z.; J.P. and J.L.B. designed, performed and analyzed studies with HBV-Env mice; A.K. generated H-*Mttp*$^{-/-}$ mice and contributed to their characterization; K.B. and C.R. performed histopathological analyses; M.M.H. and J.I. obtained purified MTP; E.B. performed PLA_2 inhibitor and siRNA studies; R.G. obtained primary HBV isolates; A.A. and J.H. contributed to human hepatocyte studies; S.S. contributed to supervision of the studies; T.J.L. and R.S.B. supervised the studies.

COMPETING FINANCIAL INTERESTS

The authors declare no competing financial interests.

Published online at http://www.nature.com/doifinder/10.1038/nm.2811.
Reprints and permissions information is available online at http://www.nature.com/reprints/index.html.

1. Thimme, R. *et al.* CD8+ T cells mediate viral clearance and disease pathogenesis during acute hepatitis B virus infection. *J. Virol.* **77**, 68–76 (2003).
2. Yeo, W. *et al.* Hepatitis B virus reactivation in lymphoma patients with prior resolved hepatitis B undergoing anticancer therapy with or without rituximab. *J. Clin. Oncol.* **27**, 605–611 (2009).
3. Esteve, M. *et al.* Chronic hepatitis B reactivation following infliximab therapy in Crohn's disease patients: need for primary prophylaxis. *Gut* **53**, 1363–1365 (2004).
4. Calabrese, L.H., Zein, N.N. & Vassilopoulos, D. Hepatitis B virus (HBV) reactivation with immunosuppressive therapy in rheumatic diseases: assessment and preventive strategies. *Ann. Rheum. Dis.* **65**, 983–989 (2006).
5. Thio, C.L. *et al.* HIV-1, hepatitis B virus, and risk of liver-related mortality in the Multicenter Cohort Study (MACS). *Lancet* **360**, 1921–1926 (2002).
6. Guidotti, L.G. & Chisari, F.V. Immunobiology and pathogenesis of viral hepatitis. *Annu. Rev. Pathol.* **1**, 23–61 (2006).
7. Bendelac, A., Savage, P.B. & Teyton, L. The biology of NKT cells. *Annu. Rev. Immunol.* **25**, 297–336 (2007).
8. Tupin, E., Kinjo, Y. & Kronenberg, M. The unique role of natural killer T cells in the response to microorganisms. *Nat. Rev. Microbiol.* **5**, 405–417 (2007).
9. Wieland, S., Thimme, R., Purcell, R.H. & Chisari, F.V. Genomic analysis of the host response to hepatitis B virus infection. *Proc. Natl. Acad. Sci. USA* **101**, 6669–6674 (2004).
10. Fisicaro, P. *et al.* Early kinetics of innate and adaptive immune responses during hepatitis B virus infection. *Gut* **58**, 974–982 (2009).
11. Webster, G.J. *et al.* Incubation phase of acute hepatitis B in man: dynamic of cellular immune mechanisms. *Hepatology* **32**, 1117–1124 (2000).
12. Guy, C.S., Mulrooney-Cousins, P.M., Churchill, N.D. & Michalak, T.I. Intrahepatic expression of genes affiliated with innate and adaptive immune responses immediately after invasion and during acute infection with woodchuck hepadnavirus. *J. Virol.* **82**, 8579–8591 (2008).
13. Kakimi, K., Guidotti, L.G., Koezuka, Y. & Chisari, F.V. Natural killer T cell activation inhibits hepatitis B virus replication in vivo. *J. Exp. Med.* **192**, 921–930 (2000).
14. Isogawa, M., Kakimi, K., Kamamoto, H., Protzer, U. & Chisari, F.V. Differential dynamics of the peripheral and intrahepatic cytotoxic T lymphocyte response to hepatitis B surface antigen. *Virology* **333**, 293–300 (2005).
15. Sprinzl, M.F., Oberwinkler, H., Schaller, H. & Protzer, U. Transfer of hepatitis B virus genome by adenovirus vectors into cultured cells and mice: crossing the species barrier. *J. Virol.* **75**, 5108–5118 (2001).
16. von Freyend, M.J. *et al.* Sequential control of hepatitis B virus in a mouse model of acute, self-resolving hepatitis B. *J. Viral Hepat.* **18**, 216–226 (2011).
17. Guidotti, L.G. *et al.* Viral clearance without destruction of infected cells during acute HBV infection. *Science* **284**, 825–829 (1999).
18. Publicover, J. *et al.* IL-21 is pivotal in determining age-dependent effectiveness of immune responses in a mouse model of human hepatitis B. *J. Clin. Invest.* **121**, 1154–1162 (2011).
19. Baron, J.L. *et al.* Activation of a nonclassical NKT cell subset in a transgenic mouse model of hepatitis B virus infection. *Immunity* **16**, 583–594 (2002).
20. Vilarinho, S., Ogasawara, K., Nishimura, S., Lanier, L.L. & Baron, J.L. Blockade of NKG2D on NKT cells prevents hepatitis and the acute immune response to hepatitis B virus. *Proc. Natl. Acad. Sci. USA* **104**, 18187–18192 (2007).
21. Brozovic, S. *et al.* CD1d function is regulated by microsomal triglyceride transfer protein. *Nat. Med.* **10**, 535–539 (2004).
22. Dougan, S.K., Rava, P., Hussain, M.M. & Blumberg, R.S. MTP regulated by an alternate promoter is essential for NKT cell development. *J. Exp. Med.* **204**, 533–545 (2007).
23. Dougan, S.K. *et al.* Microsomal triglyceride transfer protein lipidation and control of CD1d on antigen-presenting cells. *J. Exp. Med.* **202**, 529–539 (2005).
24. Kaser, A. *et al.* Microsomal triglyceride transfer protein regulates endogenous and exogenous antigen presentation by group 1 CD1 molecules. *Eur. J. Immunol.* **38**, 2351–2359 (2008).
25. Zeissig, S. *et al.* Primary deficiency of microsomal triglyceride transfer protein in human abetalipoproteinemia is associated with loss of CD1 function. *J. Clin. Invest.* **120**, 2889–2899 (2010).
26. Khatun, I. *et al.* Phospholipid transfer activity of microsomal triglyceride transfer protein produces apolipoprotein B and reduces hepatosteatosis while maintaining low plasma lipids in mice. *Hepatology* **55**, 1356–1368 (2012).
27. Ganem, D. & Prince, A.M. Hepatitis B virus infection—natural history and clinical consequences. *N. Engl. J. Med.* **350**, 1118–1129 (2004).
28. Patient, R., Hourioux, C. & Roingeard, P. Morphogenesis of hepatitis B virus and its subviral envelope particles. *Cell. Microbiol.* **11**, 1561–1570 (2009).
29. Satoh, O., Umeda, M., Imai, H., Tunoo, H. & Inoue, K. Lipid composition of hepatitis B virus surface antigen particles and the particle-producing human hepatoma cell lines. *J. Lipid Res.* **31**, 1293–1300 (1990).
30. Arrenberg, P., Halder, R., Dai, Y., Maricic, I. & Kumar, V. Oligoclonality and innate-like features in the TCR repertoire of type II NKT cells reactive to a beta-linked self-glycolipid. *Proc. Natl. Acad. Sci. USA* **107**, 10984–10989 (2010).
31. Gumperz, J.E. *et al.* Murine CD1d-restricted T cell recognition of cellular lipids. *Immunity* **12**, 211–221 (2000).
32. Cox, D. *et al.* Determination of cellular lipids bound to human CD1d molecules. *PLoS ONE* **4**, e5325 (2009).
33. Fox, L.M. *et al.* Recognition of lyso-phospholipids by human natural killer T lymphocytes. *PLoS Biol.* **7**, e1000228 (2009).
34. Ni, Z., Okeley, N.M., Smart, B.P. & Gelb, M.H. Intracellular actions of group IIA secreted phospholipase A2 and group IVA cytosolic phospholipase A2 contribute to arachidonic acid release and prostaglandin production in rat gastric mucosal cells and transfected human embryonic kidney cells. *J. Biol. Chem.* **281**, 16245–16255 (2006).
35. Ito, M. *et al.* Distribution of type V secretory phospholipase A2 expression in human hepatocytes damaged by liver disease. *J. Gastroenterol. Hepatol.* **19**, 1140–1149 (2004).
36. Masuda, S., Murakami, M., Ishikawa, Y., Ishii, T. & Kudo, I. Diverse cellular localizations of secretory phospholipase A2 enzymes in several human tissues. *Biochim. Biophys. Acta* **1736**, 200–210 (2005).

37. Kuwata, H., Yamamoto, S., Takekura, A., Murakami, M. & Kudo, I. Group IIA secretory phospholipase A2 is a unique 12/15-lipoxygenase–regulated gene in cytokine-stimulated rat fibroblastic 3Y1 cells. *Biochim. Biophys. Acta* **1686**, 15–23 (2004).
38. Tischfield, J.A. *et al.* Low-molecular-weight, calcium-dependent phospholipase A2 genes are linked and map to homologous chromosome regions in mouse and human. *Genomics* **32**, 328–333 (1996).
39. Brigl, M., Bry, L., Kent, S.C., Gumperz, J.E. & Brenner, M.B. Mechanism of CD1d-restricted natural killer T cell activation during microbial infection. *Nat. Immunol.* **4**, 1230–1237 (2003).
40. Brigl, M. *et al.* Innate and cytokine-driven signals, rather than microbial antigens, dominate in natural killer T cell activation during microbial infection. *J. Exp. Med.* **208**, 1163–1177 (2011).
41. Nagarajan, N.A. & Kronenberg, M. Invariant NKT cells amplify the innate immune response to lipopolysaccharide. *J. Immunol.* **178**, 2706–2713 (2007).
42. Fujii, S., Liu, K., Smith, C., Bonito, A.J. & Steinman, R.M. The linkage of innate to adaptive immunity via maturing dendritic cells *in vivo* requires CD40 ligation in addition to antigen presentation and CD80/86 costimulation. *J. Exp. Med.* **199**, 1607–1618 (2004).
43. Fujii, S., Shimizu, K., Smith, C., Bonifaz, L. & Steinman, R.M. Activation of natural killer T cells by α-galactosylceramide rapidly induces the full maturation of dendritic cells *in vivo* and thereby acts as an adjuvant for combined CD4 and CD8 T cell immunity to a coadministered protein. *J. Exp. Med.* **198**, 267–279 (2003).
44. Ishak, K. *et al.* Histological grading and staging of chronic hepatitis. *J. Hepatol.* **22**, 696–699 (1995).

ONLINE METHODS

Mice. CD1d-deficient, Jα18-deficient and *Tap1*$^{-/-}$ mice have been described previously[45–47]. H-*Mttp*$^{-/-}$ mice with an hepatocyte-specific deletion of the *Mttp* gene encoding microsomal triglyceride transfer protein (MTP) were generated by crossing Alb-Cre (B6.Cg-Tg(Alb-cre)21Mgn/J) mice[48] that express Cre recombinase under control of the hepatocyte-specific albumin promoter with *Mttp*$^{fl/fl}$ mice that contain loxP sites flanking *Mttp* exon 1 (ref. 49). To generate mice that allow for specific detection of noninvariant NKT cells, 4Get mice expressing GFP via an internal ribosome entry site (IRES) in the IL-4 transcript (IL-4–IRES-GFP–enhanced transcript (4Get) mice)[50,51] were crossed with CD1d-deficient and Jα18-deficient mice (see **Supplementary Data** for further information). All mice were maintained on C57BL/6J background and were backcrossed for at least eight generations. HBV-Env mice expressing the entire HBV envelope (subtype *ayw*) under control of the albumin promoter[52] were crossed with *Rag1*$^{-/-}$ and CD1d-deficient mice as described previously[19].

Primary cells and cell lines. Primary human hepatocytes were obtained from Invitrogen (Carlsbad, CA). Primary mouse hepatocytes were extracted as described previously[53]. Purity and transduction rates of primary hepatocytes are shown in **Supplementary Figure 9**. A description of all cell lines can be found in the **Supplementary Methods**.

Lipids and chemical inhibitors. Information on lipids and chemical inhibitors can be found in the **Supplementary Methods**.

Viral constructs and virus administration. The parental plasmid for HBV constructs was pGEM7-HBV1.3 containing a 1.3-fold-overlength genome of HBV, subtype *ayw*, with a 5′ terminal redundancy encompassing enhancers I and II, the origin of replication (direct repeats DR1 and DR2), the pregenomic/core promoter regions, the transcription initiation site of the pregenomic RNA, the unique polyadenylation site and the entire X open reading frame. To generate HBV mutants, point mutations were introduced using the QuickChange II site-directed mutagenesis kit and protocol (Agilent Technologies, Santa Clara, CA) at the nineteenth codon of the HBsAg pre-S1 gene from TTG to TAG (large (L) HBsAg-deficient viral mutant; L$^-$) or at the initiation codon of pre-S2 and S from ATG to GTG (middle (M) HBsAg-deficient viral mutant, M$^-$; small (S) HBsAg-deficient viral mutant, S$^-$). The pre-S1 myristylation-defective (myr$^-$) mutation was generated by changing the second codon of the pre-S1 gene from GGG (glycine) to GCG (alanine).

Additional information on virus generation and application can be found in the **Supplementary Methods**. Viral transduction rates *in vivo* and *in vitro* are shown in **Supplementary Figures 5** and **9**.

Determination of ALT, HBsAg and HBV DNA levels and liver histology. Details can be found in the **Supplementary Methods**.

Flow cytometry. Flow cytometry was performed as described previously[25]. Details can be found in the **Supplementary Methods**.

Preparation and separation of cellular and microsomal lipids. For extraction of microsomal lipids, primary hepatocytes were obtained as described above, microsomes were extracted according to methods used by Ernster *et al.*[54] and lipids were extracted following the Folch protocol[55]. Total hepatocyte lipids were extracted in a similar manner. Separation of lipids according to solubility was done as described in ref. 31. Details can be found in the **Supplementary Methods**.

Liquid chromatography–mass spectrometry. Lipid extracts were dried down, weighed and then resuspended in 95% 60:40 hexanes/isopropanol and 5% methanol (vol/vol) before mass spectrometry analyses. Twenty micrograms of lipid from each fraction was injected onto a 150 mm × 2.0 mm monochrom 3 diol column (Varian) and eluted with a gradient program in which solvent A consisted of methanol (0.1% formic acid and 0.05% ammonium hydroxide, wt/vol) and solvent B consisted of 60% hexanes and 40% isopropanol (vol/vol) (0.1% formic acid and 0.05% ammonium hydroxide wt/vol). The gradient was run from 95% to 85% solvent B from 0 to 6.6 min, to 0% solvent B until 16.2 min, and then increased back to 95% solvent B from 22.8 to 26 min. The HPLC system was an Agilent 1200 series with a 6520 quadrupole accurate mass time of flight (Q-TOF) mass spectrometer (Agilent Technologies, Santa Clara, CA), with the voltage 3.5 kV, source temperature 325 °C, drying gas 5 l/min, nebulizer pressure 30 p.s.i., running in the negative ion mode. Collision experiments were carried out by subjecting target ions to 25 eV in the collision cell. Data analysis was performed using Agilent Qualitative Analysis Mass Hunter Software Version B.03.01.

Antigen presentation. Antigen presentation assays were performed in 96-well flat-bottom plates using 2×10^4 hepatocytes, 5×10^4 RMA-S/d cells, 1×10^5 splenocytes or hepatic mononuclear cells and, as responders, 1×10^5 NKT cells or NKT cell hybridoma cells. Cytokine secretion was determined by ELISA after 16 h of coculture (BD Biosciences). In some experiments, MTP inhibitors were added at a final concentration of 10 μM (BMS212122, BMS200150) and 100 nM (BMS197636). Alternatively, purified monoclonal CD1d-blocking antibodies (1B1 clone, 19G11 clone) were used at a final concentration of 10 μg/ml.

For cell-free antigen-presentation assays, monomeric mouse CD1d (NIH Tetramer Core Facility) was loaded onto 96-well flat-bottom plates (0.25 μg per well), unbound CD1d was washed off and lipids were added at a molar ratio of 40:1. Unbound lipids were then washed off, NKT cells were added and cytokine secretion was determined by ELISA as described above. In some experiments, MTP purified from bovine liver (M.M.H.) was added at a final concentration of 500 ng/ml. In addition, in some experiments, GFP$^+$ αGalCer–CD1d-tetramer$^+$ 4Get invariant NKT cells and GFP$^+$ 4Get × Jα18-deficient noninvariant NKT cells were sorted from liver mononuclear cells using a BD Biosciences FACSAria II cell sorter and were used as responders in antigen presentation assays. Flow cytometric determination of cell surface CD69 and intracellular IFN-γ expression on GFP$^+$CD3$^+$ NKT cells was studied as readout. For *in vitro* neutralization of IL-12, a monoclonal anti–IL-12 p40 antibody (clone C17.8, eBioscience) was used at a final concentration of 10 μg/ml.

Details of ELISPOT assays can be found in the **Supplementary Methods**.

Protein extraction and western blotting. Protein extraction and western blotting were performed as described previously[25]. A detailed description can be found in the **Supplementary Methods**.

Real-time PCR. Real-time PCR was performed as described previously[25]. Primer sequences are listed in **Supplementary Table 1**. A detailed description can be found in the **Supplementary Methods**.

RNA interference. Inhibition of phospholipase expression was achieved by FlexiTube siRNA (Qiagen Inc., Hilden, Germany). siRNA was transfected using Lipofectamine 2000 (Invitrogen) according to the manufacturer's instructions. Downregulation of PLA_2 expression was investigated by SYBR-Green quantitative PCR 48 and 72 h after transfection. For antigen presentation assays, primary hepatocytes were infected with Ad-HBV and control viruses and were transfected with siRNA 24 h after infection. NKT cells were added 48 h after siRNA transfection, and cytokine secretion was determined after 16 h of coculture.

Statistical analyses. Data are expressed as means ± s.e.m. Statistical testing was done using the unpaired Student's *t* test. For comparisons of more than two groups, one-way analysis of variance was performed and was followed by Dunnett's correction. Statistical analyses were done using GraphPad Prism (GraphPad Software, Inc.).

Additional methods. Detailed methodology is described in the **Supplementary Methods**.

45. Smiley, S.T., Kaplan, M.H. & Grusby, M.J. Immunoglobulin E production in the absence of interleukin-4–secreting CD1-dependent cells. *Science* **275**, 977–979 (1997).
46. Cui, J. *et al.* Requirement for Vα14 NKT cells in IL-12–mediated rejection of tumors. *Science* **278**, 1623–1626 (1997).
47. Van Kaer, L., Ashton-Rickardt, P.G., Ploegh, H.L. & Tonegawa, S. TAP1 mutant mice are deficient in antigen presentation, surface class I molecules, and CD4–8$^+$ T cells. *Cell* **71**, 1205–1214 (1992).
48. Postic, C. *et al.* Dual roles for glucokinase in glucose homeostasis as determined by liver and pancreatic beta cell–specific gene knock-outs using Cre recombinase. *J. Biol. Chem.* **274**, 305–315 (1999).

49. Raabe, M. *et al.* Analysis of the role of microsomal triglyceride transfer protein in the liver of tissue-specific knockout mice. *J. Clin. Invest.* **103**, 1287–1298 (1999).
50. Mohrs, M., Shinkai, K., Mohrs, K. & Locksley, R.M. Analysis of type 2 immunity in vivo with a bicistronic IL-4 reporter. *Immunity* **15**, 303–311 (2001).
51. Stetson, D.B. *et al.* Constitutive cytokine mRNAs mark natural killer (NK) and NK T cells poised for rapid effector function. *J. Exp. Med.* **198**, 1069–1076 (2003).
52. Chisari, F.V. *et al.* Structural and pathological effects of synthesis of hepatitis B virus large envelope polypeptide in transgenic mice. *Proc. Natl. Acad. Sci. USA* **84**, 6909–6913 (1987).
53. Scapa, E.F. *et al.* Regulation of energy substrate utilization and hepatic insulin sensitivity by phosphatidylcholine transfer protein/StarD2. *FASEB J.* **22**, 2579–2590 (2008).
54. Ernster, L., Siekevitz, P. & Palade, G.E. Enzyme-structure relationships in the endoplasmic reticulum of rat liver: a morphological and biochemical study. *J. Cell Biol.* **15**, 541–562 (1962).
55. Folch, J., Lees, M. & Sloane Stanley, G.H. A simple method for the isolation and purification of total lipides from animal tissues. *J. Biol. Chem.* **226**, 497–509 (1957).

doi:10.1038/nm.2811

Hepatology Research

Hepatology Research 2012; 42: 958–965 doi: 10.1111/j.1872-034X.2012.01013.x

Original Article

Factors responsible for the discrepancy between *IL28B* polymorphism prediction and the viral response to peginterferon plus ribavirin therapy in Japanese chronic hepatitis C patients

Hiroaki Saito,[1,2] Kiyoaki Ito,[1] Masaya Sugiyama,[1] Teppei Matsui,[1] Yoshihiko Aoki,[1] Masatoshi Imamura,[1] Kazumoto Murata,[1] Naohiko Masaki,[1] Hideyuki Nomura,[3] Hiroshi Adachi,[4] Shuhei Hige,[5] Nobuyuki Enomoto,[6] Naoya Sakamoto,[7] Masayuki Kurosaki,[8] Masashi Mizokami[1] and Sumio Watanabe[2]

[1]*The Research Center for Hepatitis and Immunology, National Center for Global Health and Medicine, Ichikawa,* [2]*Department of Gastroenterology, Juntendo University School of Medicine, Bunkyoku,* [3]*The Center for Liver Diseases, Shin-Kokura Hospital, Kitakyushu, Fukuoka,* [4]*Department of Virology and Liver Unit, Tonami General Hospital, Tonami,* [5]*Department of Internal Medicine, Hokkaido University Graduate School of Medicine, Sapporo,* [6]*Department of Internal Medicine, University of Yamanashi, Kofu,* [7]*Department for Hepatitis Control, Tokyo Medical and Dental University, Tokyo, and* [8]*Division of Gastroenterology and Hepatology, Musashino Red Cross Hospital, Musashino, Japan*

Aim: IL28B polymorphisms serve to predict response to pegylated interferon plus ribavirin therapy (PEG IFN/RBV) in Japanese patients with chronic hepatitis C (CHC) very reliably. However, the prediction by the *IL28B* polymorphism contradicted the virological response to PEG IFN/RBV in some patients. Here, we aimed to investigate the factors responsible for the discrepancy between the *IL28B* polymorphism prediction and virological responses.

Methods: CHC patients with genotype 1b and high viral load were enrolled in this study. In a case–control study, clinical and virological factors were analyzed for 130 patients with rs8099917 TT genotype and 96 patients with rs8099917 TG or GG genotype who were matched according to sex, age, hemoglobin level and platelet count.

Results: Higher low-density lipoprotein (LDL) cholesterol, lower γ-glutamyltransferase and the percentage of wild-type phenotype at amino acids 70 and 91 were significantly associated with the rs8099917 TT genotype. Multivariate analysis showed that rs8099917 TG or GG genotype, older age and lower LDL cholesterol were independently associated with the non-virological responder (NVR) phenotype. In patients with rs8099917 TT genotype (predicted as virological responder [VR]), multivariate analysis showed that older age was independently associated with NVR. In patients with rs8099917 TG or GG genotype (predicted as NVR), multivariate analysis showed that younger age was independently associated with VR.

Conclusion: Patient age gave rise to the discrepancy between the prediction by *IL28B* polymorphism and the virological responses, suggesting that patients should be treated at a younger age.

Key words: aging, genotype, IL28B, low-density lipoprotein cholesterol, single nucleotide polymorphism

INTRODUCTION

HEPATITIS C VIRUS (HCV) infection is a global health problem with worldwide estimates of 120–130 million carriers.[1] Chronic HCV infection, the leading cause of liver transplantation, can lead to progressive liver disease, resulting in cirrhosis and complications, including decompensated liver disease and hepatocellular carcinoma.[2] The current standard-of-care treatment for suitable patients with chronic HCV infection consists of pegylated interferon-α-2a or -2b (PEG IFN) given by injection in combination with oral ribavirin (RBV) for 24 or 48 weeks, depending on HCV genotype. Large-scale treatment in the USA and Europe showed that 42–52% of patients with HCV genotype 1

Correspondence: Dr Masashi Mizokami, The Research Center for Hepatitis and Immunology, National Center for Global Health and Medicine, 1-7-1 Kohnodai, Ichikawa, Chiba 272-8516, Japan. Email: mmizokami@hospk.ncgm.go.jp
Received 23 February 2012; revision 18 March 2012; accepted 22 March 2012.

achieved a sustained virological response (SVR),[3–5] and studies conducted in Japan produced similar results. This treatment is associated with well-known side-effects (e.g. influenza-like syndrome, hematological abnormalities and neuropsychiatric events) resulting in reduced compliance and fewer patients completing treatment.[6] It is important to predict an individual's response before treatment with PEG IFN/RBV to avoid side-effects, as well as to reduce the treatment cost. The HCV genotype, in particular, is used to predict the response: patients with the HCV genotype 2/3 have a relatively high rate of SVR (70–80%) with 24 weeks of treatment, whereas those infected with genotype 1 have a much lower rate of SVR, despite 48 weeks of treatment.[5]

Our recent genome-wide association studies (GWAS) revealed that several highly correlated common single nucleotide polymorphisms (SNP) in the region of the interleukin-28B (*IL28B*) gene on chromosome 19, coding for interferon (IFN)-λ3, are implicated in the non-virological responder (NVR) to PEG IFN/RBV phenotype among patients infected by HCV genotype 1.[7] The association between response to PEG IFN/RBV and SNP associated with *IL28B* was concurrently reported by two other groups who also employed GWAS.[8,9] The *IL28B* polymorphism was highly predictive of the response to PEG IFN/RBV therapy in Japanese chronic hepatitis C (CHC) patients.[10–12] However, this was not always the case. Therefore, we attempted to determine why the *IL28B* polymorphism did not predict the response of all patients. The nature of the functional link between the *IL28B* polymorphism and HCV clearance is unknown, and this must be defined to understand how the *IL28B* polymorphism correlates with HCV clearance. Therefore, we also investigated the association between the *IL28B* polymorphism and clinical characteristics of CHC patients.

METHODS

Patients

A TOTAL OF 696 CHC patients with genotype 1b and high viral load were recruited from the National Center for Global Health and Medicine, Hokkaido University Hospital, Tokyo Medical and Dental University Hospital, Yamanashi University Hospital, Tonami General Hospital, and Shin-Kokura Hospital in Japan. In a case–control study, sex, age, hemoglobin level and platelet count were matched between patients with the rs8099917 TT genotype ($n = 130$) and patients with rs8099917 TG or GG genotypes ($n = 96$) to eliminate background biases.

Each patient was treated with PEG IFN-α-2b (1.5 μg/kg s.c. weekly) or PEG IFN-α-2a (180 μg/body s.c. weekly) plus RBV (600–1000 mg daily, depending on bodyweight). Because a reduction in the dose of PEG IFN/RBV can contribute to a lower SVR rate,[13] only patients with an adherence of more than 80% dose for both drugs during the first 12 weeks were included in this study. Those positive for hepatitis B surface antigen and/or anti-HIV were excluded from this study.

Non-virological response was defined as less than a 2 log-unit decline in the serum level of HCV RNA from the pretreatment baseline value within the first 12 weeks and detectable viremia 24 weeks after treatment. Virological response (VR) was defined as attaining SVR or transient virological response (TVR) in this study; SVR was defined as undetectable HCV RNA in serum 6 months after treatment, whereas TVR was defined as a reappearance of HCV RNA in serum after the treatment was discontinued for a patient who had undetectable HCV RNA during the therapy or on completion of the therapy. At the time of enrollment, written informed consent was obtained for the collection and storage of serum and peripheral blood. This study was conducted in accordance with provisions of the Declaration of Helsinki.

Clinical and laboratory data

The sex, age, hemoglobin (Hb) and platelet counts were matched between study groups. Other parameters determined were as follows: alkaline phosphatase (ALP), alanine transaminase (ALT), total cholesterol, fasting blood sugar (FBS), low-density lipoprotein (LDL) cholesterol, γ-glutamyl transpeptidase (γ-GTP), α-fetoprotein (AFP), HCV RNA level and the rs8099917 polymorphism near *IL28B*.

DNA extraction

Genomic DNA was extracted from the buffy coat fraction of patients' whole blood using a GENOMIX kit (Talent SRL; Trieste, Italy).

IL28B genotyping

We have reported that the rs8099917 polymorphism is the best predictor for the response of Japanese CHC patients to PEG IFN/RBV therapy than other SNP near *IL28B*.[14] Therefore, the rs8099917 polymorphism was genotyped using the InvaderPlus assay (Third Wave Japan, Tokyo, Japan), which combines polymerase

chain reaction (PCR) and the invader reaction.[15,16] The InvaderPlus assay was performed using the LightCycler LC480 (Roche Applied Science, Mannheim, Germany).

Detection of amino acid substitutions in core and NS5A regions of HCV-1b

In the present study, substitutions of amino acid residues 70 (s-aa 70) and 91 (s-aa 91), and the presence of the IFN sensitivity-determining region (ISDR) were determined by direct nucleotide sequencing. HCV RNA was extracted from serum samples at the start of patients' therapy and reverse transcribed with a random primer and SuperScript III reverse transcriptase (Life Technologies, Carlsbad, CA, USA). Nucleic acids were amplified by PCR as described.[17]

Statistical analysis

Quantitative variables were expressed as the mean ± standard error (SE) unless otherwise specified. Categorical variables were compared using a χ^2-test or Fisher's exact test, as appropriate, and continuous variables were compared using the Mann–Whitney *U*-test. $P < 0.05$ was considered statistically significant. Multivariate analysis was performed using a stepwise logistic regression model. We performed statistical analyses using STATA ver. 11.0 (StataCorp, College Station, TX, USA).

RESULTS

Patient characteristics and *IL28B* genotype in a matched case–control study

TABLE 1 SHOWS PATIENT characteristics according to *IL28B* genotype. In a matched case–control study, sex, age, Hb levels and platelet counts were matched between 130 patients with rs8099917 TT genotype and 96 patients with rs8099917 TG or GG genotype. Lower γ-GTP ($P = 0.013$) and higher LDL cholesterol levels ($P < 0.001$) were significantly associated with the TT genotype of rs8099917. The percentages of wild type of s-aa 70 and s-aa 91 of patients with the rs8099917 TT genotype were significantly higher than those of patients with rs8099917 TG or GG genotype (s-aa 70: TT vs TG + GG, 68% vs 37% [$P < 0.001$]; s-aa 91: TT vs TG + GG, 68% vs 51% [$P = 0.017$]).

Factors associated with NVR in total patients

Table 2 shows the factors associated with NVR by univariate and multivariate analyses. Univariate analysis showed that older age ($P = 0.002$), lower platelet counts ($P = 0.01$), higher γ-GTP ($P = 0.013$), lower total cholesterol ($P = 0.017$), lower LDL cholesterol ($P < 0.001$) levels and higher AFP levels ($P = 0.019$) were significantly associated with NVR. The percentage of TG or GG genotype of rs8099917 of patients with NVR was

Table 1 Univariate analysis of *IL28B* TT and TG + GG genotypes

Variable	TT genotype ($n = 130$)	TG + GG genotype ($n = 96$)	*P*-value
Sex (% male)	61 (47)	46 (48)	Matched
Age (years), mean (SE)	57.2 (0.8)	57.5 (0.9)	Matched
Hemoglobin (g/dL), mean (SE)	14.3 (0.3)	13.9 (0.2)	Matched
Platelet count (/μL), mean (SE)	16.2 (0.5)	16.0 (0.5)	Matched
ALT (IU/L), mean (SE)	79.4 (5.4)	80.5 (7.8)	0.281
ALP (IU/L), mean (SE)	273.8 (11.7)	283.9 (11.8)	0.313
γ-GTP (IU/L), mean (SE)	63.4 (6.0)	76.0 (6.4)	0.013
Total cholesterol (mg/dL), mean (SE)	177.5 (3.3)	172.3 (3.2)	0.345
LDL cholesterol (mg/dL), mean (SE)	99.0 (2.6)	83.5 (2.8)	<0.001
Fasting blood sugar (mg/dL), mean (SE)	114.1 (4.1)	104.4 (1.9)	0.97
AFP (ng/dL), mean (SE)	9.8 (1.1)	11.5 (1.6)	0.190
HCV RNA (log IU), mean (SE)	6.2 (0.1)	6.1 (0.1)	0.186
s-aa 70 wild type (%)	70/103 (68)	30/81 (37)	<0.001
s-aa 91 wild type (%)	70/103 (68)	41/81 (51)	0.017
ISDR mutation 0–1 point (%)	82/100 (82)	70/81 (86)	0.42

AFP, α-fetoprotein; ALP, alkaline phosphatase; ALT, alanine aminotransferase; γ-GTP, γ-glutamyl transpeptidase; HCV, hepatitis C virus; ISDR, interferon sensitivity-determining region; LDL, low-density lipoprotein; SE, standard error.

Table 2 Univariate and multivariate analyses of patients with chronic hepatitis C treated with PEG IFN/RBV with respect to VR and NVR

Variable	Univariate analysis			Multivariate analysis	
	VR ($n = 128$)	NVR ($n = 98$)	*P*-value	OR (95% CI)	*P*-value
Sex (% male)	65 (51)	42 (43)	0.237		
Age (years), mean (SE)	55.6 (0.8)	59.6 (0.9)	0.002	1.075 (1.012–1.143)	0.02
rs8099917 (TG or GG genotype) (%)	23/128 (18)	73/98 (74)	<0.001	25.460 (7.436–87.169)	<0.001
Hemoglobin (g/dL), mean (SE)	14.4 (0.3)	13.7 (0.2)	0.053		
Platelet count (/μL), mean (SE)	16.9 (0.5)	15.0 (0.5)	0.01		
ALT (IU/L), mean (SE)	83.9 (6.4)	74.5 (6.2)	0.116		
ALP (IU/L), mean (SE)	274.1 (12.3)	282.9 (11.2)	0.169		
γ-GTP (IU/L), mean (SE)	65.9 (6.4)	72.6 (5.6)	0.013		
Total cholesterol (mg/dL), mean (SE)	180.3 (3.1)	168.4 (3.5)	0.017		
LDL cholesterol (mg/dL), mean (SE)	100.5 (2.7)	83.5 (2.8)	<0.001	0.978 (0.956–0.999)	0.046
Fasting blood sugar (mg/dL), mean (SE)	106.6 (2.9)	114.8 (4.4)	0.058		
AFP (ng/dL), mean (SE)	9.6 (1.1)	12.0 (1.6)	0.021		
HCV RNA (Log IU), mean (SE)	6.2 (0.1)	6.2 (0.1)	0.876		
s-aa 70 wild type (%)	67/102 (66)	33/82 (54)	0.001		
s-aa 91 wild type (%)	67/102 (66)	44/82 (54)	0.097		
ISDR mutation 0–1 point (%)	79/96 (82)	73/85 (86)	0.511		

AFP, α-fetoprotein; ALP, alkaline phosphatase; ALT, alanine aminotransferase; CI, confidence interval; γ-GTP, γ-glutamyl transpeptidase; HCV, hepatitis C virus; ISDR, interferon sensitivity-determining region; LDL, low-density lipoprotein; NVR, non-virological response; OR, odds ratio; PEG IFN, peginterferon; SE, standard error; RBV, ribavirin; VR, virological response.

significantly higher than that of patients with VR (VR vs NVR: 23/128 [18%] vs 73/98 [74%], $P < 0.001$). The percentage of wild-type s-aa 70 in patients with NVR was significantly lower than that in patients with VR [VR vs NVR: 67/102 [66%] vs 33/82 [54%], $P = 0.001$]. Multivariate analysis showed that older age (odds ratio [OR] = 1.075; 95% confidence interval [CI] = 1.012–1.14; $P = 0.02$), TG or GG genotype of rs8099917 (OR = 25.460; 95% CI = 7.436–87.169; $P < 0.001$) and lower LDL cholesterol levels (OR = 0.978; 95% CI = 0.956–0.999; $P = 0.046$) were independently associated with NVR.

VR to treatment depending on *IL28B* genotype

In the patients with the rs8099917 TT genotype, the rates of SVR, TVR and NVR were 62%, 19% and 19%, respectively. Therefore, 19% patients were NVR, even though rs8099917 represents the TT genotype (predicted as VR). In contrast, in the patients with rs8099917 TG or GG, the rates of SVR, TVR and NVR were 14%, 10% and 76%, respectively. Therefore, 24% patients were VR, even though rs8099917 was TG or GG genotype (predicted as NVR) (Fig. 1).

Factors associated with NVR in patients with the rs8099917 TT genotype

Table 3 shows the factors associated with NVR in patients with the rs8099917 TT genotype (predicted as VR) by univariate and multivariate analyses. Univariate analysis showed that female sex ($P = 0.003$), older age

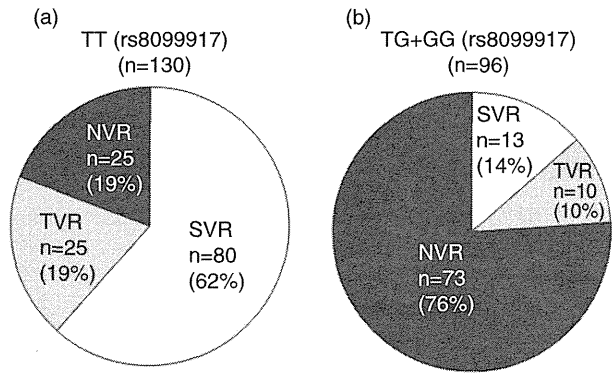

Figure 1 Virological responses to pegylated interferon and ribavirin therapy were shown in patients with rs8099917 TT (a) and TG + GG (b). NVR, non-virological response; SVR, sustained virological response; TVR, transient virological response.

Table 3 Variables associated with NVR by univariate and multivariate analyses in patients with rs8099917 TT genotype

Variable	Univariate analysis			Multivariate analysis	
	VR ($n = 105$)	NVR ($n = 25$)	*P*-value	OR (95% CI)	*P*-value
Sex (% male)	56 (53)	5 (20)	0.003		
Age (years), mean (SE)	56.1 (0.8)	61.7 (1.6)	0.001	1.142 (1.026–1.271)	0.015
Hemoglobin (g/dL), mean (SE)	14.6 (0.4)	13.1 (0.3)	0.005		
Platelet count (/μL), mean (SE)	16.7 (0.6)	13.8 (1.0)	0.019		
ALT (IU/L), mean (SE)	83.6 (6.3)	61.0 (7.9)	0.053		
ALP (IU/L), mean (SE)	270.6 (13.6)	285.9 (22.3)	0.206		
γ-GTP (IU/L), mean (SE)	66.9 (7.1)	49.2 (7.4)	0.473		
Total cholesterol (mg/dL), mean (SE)	180.2 (3.6)	165.0 (7.6)	0.072		
LDL cholesterol (mg/dL), mean (SE)	101.2 (2.9)	88.5 (5.2)	0.067		
Fasting blood sugar (mg/dL), mean (SE)	108.4 (3.5)	140.0 (15.5)	0.127		
AFP (ng/dL), mean (SE)	9.4 (1.2)	12.2 (3.6)	0.245		
HCV RNA (log IU), mean (SE)	6.2 (0.1)	6.2 (0.1)	0.948		
s-aa 70 wild type (%)	57/83 (66)	13/20 (75)	0.752		
s-aa 91 wild type (%)	55/83 (66)	15/20 (75)	0.452		
ISDR mutation 0–1 point (%)	64/79 (81)	18/21 (86)	0.618		

AFP, α-fetoprotein; ALP, alkaline phosphatase; ALT, alanine aminotransferase; CI, confidence interval; γ-GTP, γ-glutamyl transpeptidase; HCV, hepatitis C virus; ISDR, interferon sensitivity-determining region; LDL, low-density lipoprotein; NVR, non-virological response; OR, odds ratio; SE, standard error; VR, virological response.

($P = 0.001$), lower Hb levels ($P = 0.005$) and lower platelet counts ($P = 0.019$) were significantly associated with NVR in patients with the rs8099917 TT genotype. Multivariate analysis showed that only older age was independently associated with NVR in patients with the rs8099917 TT genotype (predicted as VR) (OR = 1.142; 95% CI = 1.026–1.27; $P = 0.015$).

Factors associated with VR in patients with the rs8099917 TG or GG genotypes

Table 4 shows the factors associated with VR in patients with the rs8099917 TG or GG genotypes (predicted as NVR) by univariate and multivariate analyses. Younger age ($P = 0.005$), lower γ-GTP ($P = 0.009$) and higher LDL cholesterol levels ($P = 0.032$) were significantly associated with VR by univariate analysis. Multivariate analysis showed that only younger age was independently associated with VR in patients with the rs8099917 TG or GG genotype (predicted as NVR) (OR = 0.926; 95% CI = 0.867–0.990; $P = 0.023$).

Rate of VR depending on the rs8099917 genotype of each age group

We divided patients into four age groups and compared VR rates by the differences in rs8099917 genotype for each group. The rate of VR decreased gradually in the older age groups independent of genotype. In the less than 49 years age group, the rate of VR in patients with the rs8099917 TT genotype was significantly higher than that in patients with the rs8099917 TG + GG genotypes ($P = 0.0002$). Further, in the 50–59 and 60–69 years age groups, the rates of VR in patients with the rs8099917 TT genotype were significantly higher than those in patients with the rs8099917 TG + GG genotypes ($P < 0.0001$, respectively). In the group that included subjects aged older than 69 years, only 50% of patients achieved VR even in those with the rs8099917 TT genotype (predicted as VR). In contrast, 47.6% of patients achieved VR, including those with the rs8099917 TG or GG genotypes (predicted as NVR) in the less than 49 years group (Fig. 2).

DISCUSSION

SINGLE NUCLEOTIDE POLYMORPHISM array analysis employing GWAS technology conducted by our laboratory and others revealed the relationships between SNP associated with the *IL28B* locus or present within the coding sequences for IFN-λ3, or the response to PEG IFN/RBV therapy for CHC.[7–9] Subsequent studies have confirmed that the response to PEG IFN/RBV therapy correlates with the SNP associated with *IL28B*[18,19] and indicates their value for predicting the response to PEG IFN/RBV therapy. Unfortunately, these predictions do not hold for some patients. In an attempt to understand the reasons for this, in the present study,

Table 4 Variables associated with VR by univariate and multivariate analyses in patients with rs8099917 TG or GG genotypes

Variable	Univariate analysis			Multivariate analysis	
	VR ($n = 23$)	NVR ($n = 73$)	*P*-value	OR (95% CI)	*P*-value
Sex (% male)	9 (40%)	37 (51%)	0.333		
Age (years), mean (SE)	53.2 (1.7)	58.8 (1.1)	0.005	0.926 (0.867–0.990)	0.023
Hemoglobin (g/dL), mean (SE)	13.6 (0.3)	13.9 (0.2)	0.44		
Platelet count (/μL), mean (SE)	17.6 (1.1)	15.5 (0.6)	0.059		
ALT (IU/L), mean (SE)	85.5 (21.6)	78.9 (7.8)	0.767		
ALP (IU/L), mean (SE)	291.9 (28.6)	281.8 (13.0)	0.921		
γ-GTP (IU/L), mean (SE)	62.2 (15.1)	80.4 (6.9)	0.009		
Total cholesterol (mg/dL), mean (SE)	180.5 (6.2)	169.5 (3.7)	0.17		
LDL cholesterol (mg/dL), mean (SE)	97.6 (6.9)	81.9 (3.6)	0.032		
Fasting blood sugar (mg/dL), mean (SE)	98.1 (2.8)	106.3 (2.3)	0.084		
AFP (ng/dL), mean (SE)	10.3 (3.4)	11.9 (1.8)	0.123		
HCV RNA (log IU), mean (SE)	5.9 (0.1)	6.2 (0.1)	0.087		
s-aa 70 wild type (%)	10/19 (53)	20/62 (32)	0.108		
s-aa 91 wild type (%)	12/19 (63)	29/62 (47)	0.211		
ISDR mutation 0–1 point (%)	15/17 (88)	55/64 (86)	0.806		

AFP, α-fetoprotein; ALP, alkaline phosphatase; ALT, alanine aminotransferase; CI, confidence interval; γ-GTP, γ-glutamyl transpeptidase; HCV, hepatitis C virus; ISDR, interferon sensitivity-determining region; LDL, low-density lipoprotein; NVR, non-virological response; OR, odds ratio; SE, standard error; VR, virological response.

we recruited a new set of patients for further analysis. Here, we confirmed that *IL28B* polymorphism was the most significant predictive factor for NVR with respect to PEG IFN/RBV treatment. Moreover, 19% of patients exhibiting the rs8099917 TT genotype were NVR, although they were predicted as VR. Twenty-four percent of patients with the rs8099917 TG or GG genotypes were VR, although they were predicted as NVR. We were able to determine by multivariate analysis that age was the most likely factor responsible for the discordance

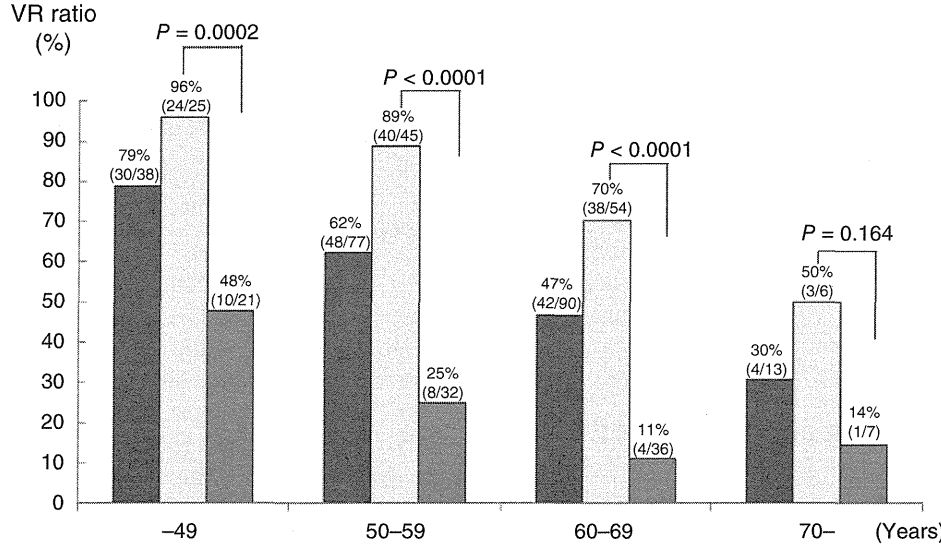

Figure 2 Virological responses (VR) to pegylated interferon and ribavirin therapy were compared between the patients with rs8099917 TT and TG + GG in each generation group. (■) Total patients, (□) TT genotype (rs8099917), (▣) TG + GG genotype (rs8099917).

between *IL28B* genotype and patients' response to viral infection.

How does age influence the VR to PEG IFN/RBV therapy? First, the lower rate of VR to PEG IFN/RBV therapy in patients with CHC was attributed to lower compliance with the IFN or RBV dose.[20,21] Because lower compliance with PEG IFN or RBV therapy was expected to be associated with a lower rate of VR in older patients, we recruited patients who were administrated over 80% of the prescribed dose of IFN/RBV. Therefore, lower compliance can be discounted as a reason for reduced response. Second, a more advanced stage of fibrosis might have been present in the older group. Platelet counts in patients with NVR were significantly lower than those in patients with VR, and lower platelet counts may be associated with advanced fibrosis.[22] Moreover, advanced fibrosis is associated with lower rates of SVR to IFN-based therapy.[23] Third, epigenetic factors such as DNA methylation induced by aging may be involved in the reduced efficacy of PEG IFN/RBV treatment in older patients. DNA methylation near gene promoters is known to turn off transcription or reduce it considerably,[24] and advanced age is strongly associated with the increased DNA methylation.[25] Therefore, DNA methylation may be increased near or in the *IL28B* promoter as a function of age resulting in suppression of *IL28B* transcription.

Lower LDL cholesterol levels were significantly associated with NVR in patients with CHC. Moreover, LDL cholesterol levels in patients with the rs8099917 TT genotype were significantly higher than those in patients with the TG + GG genotypes. The association between LDL cholesterol and *IL28B* polymorphism as well as the VR to PEG IFN/RBV has been reported.[26] Higher pretreatment levels of LDL cholesterol have been shown to predict increased response to standard PEG IFN/RBV treatment for patients with CHC.[27,28] Although the mechanisms responsible for the association between LDL cholesterol levels and the VR to PEG IFN/RBV are unknown, the *IL28B*-rs8099917 TT responder genotype, which may correlate with an increased likelihood of treatment response and higher LDL cholesterol levels, is associated with either lower IFN-λ3 activity or reduced expression of genes regulated by IFN-mediated signaling pathways.

In conclusion, our studies provide compelling evidence that patient age is most likely responsible for incorrect predictions of VR to PEG IFN/RBV therapy in Japanese CHC patients based on *IL28B* genotypes. Our findings indicated that patients should be treated as soon as they are diagnosed. It will be important to investigate the role of the epigenetic factors associated with *IL28B* expression to develop more effective PEG IFN/RBV-based therapies for patients with CHC.

ACKNOWLEDGMENT

THIS STUDY WAS supported by grants (21–112 and 21–113) from the National Center for Global Health and Medicine in Japan.

REFERENCES

1 Global Burden of Hepatitis C Working Group. Global burden of disease (GBD) for hepatitis C. *J Clin Pharmacol* 2004; **44**: 20–9.
2 Younossi Z, Kallman J, Kincaid J. The effects of HCV infection and management on health-related quality of life. *Hepatology* 2007; **45**: 806–16.
3 Fried MW, Shiffman ML, Reddy KR *et al.* Peginterferon alfa-2a plus ribavirin for chronic hepatitis C virus infection. *N Engl J Med* 2002; **347**: 975–82.
4 Manns MP, McHutchison JG, Gordon SC *et al.* Peginterferon alfa-2b plus ribavirin compared with interferon alfa-2b plus ribavirin for initial treatment of chronic hepatitis C: a randomised trial. *Lancet* 2001; **358**: 958–65.
5 Hadziyannis SJ, Sette H, Jr, Morgan TR *et al.* Peginterferon-alpha2a and ribavirin combination therapy in chronic hepatitis C: a randomized study of treatment duration and ribavirin dose. *Ann Intern Med* 2004; **140**: 346–55.
6 Bruno S, Camma C, Di Marco V *et al.* Peginterferon alfa-2b plus ribavirin for naive patients with genotype 1 chronic hepatitis C: a randomized controlled trial. *J Hepatol* 2004; **41**: 474–81.
7 Tanaka Y, Nishida N, Sugiyama M *et al.* Genome-wide association of IL28B with response to pegylated interferon-alpha and ribavirin therapy for chronic hepatitis C. *Nat Genet* 2009; **41**: 1105–9.
8 Ge D, Fellay J, Thompson AJ *et al.* Genetic variation in IL28B predicts hepatitis C treatment-induced viral clearance. *Nature* 2009; **461**: 399–401.
9 Suppiah V, Moldovan M, Ahlenstiel G *et al.* IL28B is associated with response to chronic hepatitis C interferon-alpha and ribavirin therapy. *Nat Genet* 2009; **41**: 1100–4.
10 Watanabe S, Enomoto N, Koike K *et al.* Cancer preventive effect of pegylated interferon alpha-2b plus ribavirin in a real-life clinical setting in Japan: PERFECT interim analysis. *Hepatol Res* 2011; **41**: 955–64.
11 Kurosaki M, Tanaka Y, Nishida N *et al.* Pre-treatment prediction of response to pegylated-interferon plus ribavirin for chronic hepatitis C using genetic polymorphism in IL28B and viral factors. *J Hepatol* 2011; **54**: 439–48.
12 Kurosaki M, Sakamoto N, Iwasaki M *et al.* Pretreatment prediction of response to peginterferon plus ribavirin

therapy in genotype 1 chronic hepatitis C using data mining analysis. *J Gastroenterol* 2011; **46**: 401–9.
13 McHutchison JG, Manns M, Patel K *et al.* Adherence to combination therapy enhances sustained response in genotype-1-infected patients with chronic hepatitis C. *Gastroenterology* 2002; **123**: 1061–9.
14 Ito K, Higami K, Masaki N *et al.* The rs8099917 polymorphism, when determined by a suitable genotyping method, is a better predictor for response to pegylated alpha interferon/ribavirin therapy in Japanese patients than other single nucleotide polymorphisms associated with interleukin-28B. *J Clin Microbiol* 2011; **49**: 1853–60.
15 Lyamichev V, Mast AL, Hall JG *et al.* Polymorphism identification and quantitative detection of genomic DNA by invasive cleavage of oligonucleotide probes. *Nat Biotechnol* 1999; **17**: 292–6.
16 Lyamichev VI, Kaiser MW, Lyamicheva NE *et al.* Experimental and theoretical analysis of the invasive signal amplification reaction. *Biochemistry* 2000; **39**: 9523–32.
17 Akuta N, Suzuki F, Hirakawa M *et al.* Amino acid substitution in hepatitis C virus core region and genetic variation near the interleukin 28B gene predict viral response to telaprevir with peginterferon and ribavirin. *Hepatology* 2010; **52**: 421–9.
18 Rauch A, Kutalik Z, Descombes P *et al.* Genetic variation in IL28B is associated with chronic hepatitis C and treatment failure: a genome-wide association study. *Gastroenterology* 2010; **138**: 1338–45. 45 e1–7.
19 Montes-Cano MA, Garcia-Lozano JR, Abad-Molina C *et al.* Interleukin-28B genetic variants and hepatitis virus infection by different viral genotypes. *Hepatology* 2010; **52**: 33–7.
20 Yamada G, Iino S, Okuno T *et al.* Virological response in patients with hepatitis C virus genotype 1b and a high viral load: impact of peginterferon-alpha-2a plus ribavirin dose reductions and host-related factors. *Clin Drug Investig* 2008; **28**: 9–16.
21 Bourliere M, Ouzan D, Rosenheim M *et al.* Pegylated interferon-alpha2a plus ribavirin for chronic hepatitis C in a real-life setting: the Hepatys French cohort (2003–2007). *Antivir Ther* 2012; **17**: 101–10.
22 Karasu Z, Tekin F, Ersoz G *et al.* Liver fibrosis is associated with decreased peripheral platelet count in patients with chronic hepatitis B and C. *Dig Dis Sci* 2007; **52**: 1535–9.
23 Everson GT, Hoefs JC, Seeff LB *et al.* Impact of disease severity on outcome of antiviral therapy for chronic hepatitis C: lessons from the HALT-C trial. *Hepatology* 2006; **44**: 1675–84.
24 Suzuki MM, Bird A. DNA methylation landscapes: provocative insights from epigenomics. *Nat Rev Genet* 2008; **9**: 465–76.
25 Boks MP, Derks EM, Weisenberger DJ *et al.* The relationship of DNA methylation with age, gender and genotype in twins and healthy controls. *PLoS ONE* 2009; **4**: e6767.
26 Li JH, Lao XQ, Tillmann HL *et al.* Interferon-lambda genotype and low serum low-density lipoprotein cholesterol levels in patients with chronic hepatitis C infection. *Hepatology* 2010; **51**: 1904–11.
27 Gopal K, Johnson TC, Gopal S *et al.* Correlation between beta-lipoprotein levels and outcome of hepatitis C treatment. *Hepatology* 2006; **44**: 335–40.
28 Toyoda H, Kumada T. Cholesterol and lipoprotein levels as predictors of response to interferon for hepatitis C. *Ann Intern Med* 2000; **133**: 921.

HEPATOLOGY
Official Journal of the American Association for the Study of Liver Diseases

LecT-Hepa, a Glyco-Marker Derived from Multiple Lectins, as a Predictor of Liver Fibrosis in Chronic Hepatitis C Patients

Kiyoaki Ito,[1] Atsushi Kuno,[2] Yuzuru Ikehara,[2] Masaya Sugiyama,[1] Hiroaki Saito,[1] Yoshihiko Aoki,[1] Teppei Matsui,[1] Masatoshi Imamura,[1] Masaaki Korenaga,[1] Kazumoto Murata,[1] Naohiko Masaki,[1] Yasuhito Tanaka,[3] Shuhei Hige,[4] Namiki Izumi,[5] Masayuki Kurosaki,[5] Shuhei Nishiguchi,[6] Michiie Sakamoto,[7] Masayoshi Kage,[8] Hisashi Narimatsu,[2] and Masashi Mizokami[1]

Assessment of liver fibrosis in patients with chronic hepatitis C (CHC) is critical for predicting disease progression and determining future antiviral therapy. LecT-Hepa, a new glyco-marker derived from fibrosis-related glyco-alteration of serum alpha 1-acid glycoprotein, was used to differentiate cirrhosis from chronic hepatitis in a single-center study. Herein, we aimed to validate this new glyco-marker for estimating liver fibrosis in a multicenter study. Overall, 183 CHC patients were recruited from 5 liver centers. The parameters *Aspergillus oryzae* lectin (AOL) / *Dature stramonium* lectin (DSA) and *Maackia amurensis* lectin (MAL)/DSA were measured using a bedside clinical chemistry analyzer in order to calculate LecT-Hepa levels. The data were compared with those of seven other noninvasive biochemical markers and tests (hyaluronic acid, tissue inhibitor of metalloproteases-1, platelet count, aspartate aminotransferase-to-platelet ratio index [APRI], Forns index, Fib-4 index, and Zeng's score) for assessing liver fibrosis using the receiver-operating characteristic curve. LecT-Hepa correlated well with the fibrosis stage as determined by liver biopsy. The area under the curve (AUC), sensitivity, and specificity of LecT-Hepa were 0.802, 59.6%, and 89.9%, respectively, for significant fibrosis; 0.882, 83.3%, and 80.0%, respectively, for severe fibrosis; and 0.929, 84.6%, and 88.5%, respectively, for cirrhosis. AUC scores of LecT-Hepa at each fibrosis stage were greater than those of the seven aforementioned noninvasive tests and markers. *Conclusion*: The efficacy of LecT-Hepa, a glyco-marker developed using glycoproteomics, for estimating liver fibrosis was demonstrated in a multicenter study. LecT-Hepa given by a combination of the two glyco-parameters is a reliable method for determining the fibrosis stage and is a potential substitute for liver biopsy. (HEPATOLOGY 2012;56:1448-1456)

Accurate staging of hepatic fibrosis in patients with chronic hepatitis C (CHC) is most important for predicting disease progression and determining the need for initiating antiviral therapy, such as interferon (IFN) therapy.[1,2] Liver biopsy has been considered the gold standard for fibrosis staging for many years.[3] However, liver biopsy is invasive and painful,[4,5] with rare but potentially life-threatening complications.[6] In addition, this method may suffer from sampling errors since only 1/50,000 of the organ is examined.[7] Furthermore, inter- and intraobserver discrepancies reaching levels of 10% to 20% have been

Abbreviations: α2-MG, α2-macroglobulin; AFP, alpha-fetoprotein; AGP, alpha-1 acid glycoprotein; ALT, alanine aminotransferase; AOL, Aspergillus oryzae *lectin; CHC, chronic hepatitis C; DSA,* Datura stramonium *lectin; GGT, gamma-glutamyltransferase; HA, hyaluronic acid; HCC, hepatocellular carcinoma; HCV, hepatitis C virus; IFN, interferon; MAL,* Maackia amurensis *lectin; TIMP1, tissue inhibitors of metalloproteinases 1.*

From the [1]Research Center for Hepatitis and Immunology, National Center for Global Health and Medicine, Ichikawa, Japan; [2]Research Center for Medical Glycoscience, National Institute of Advanced Industrial Science and Technology, Tsukuba, Japan; [3]Department of Virology & Liver Unit, Nagoya City University Graduate School of Medical Sciences, Nagoya, Japan; [4]Department of Internal Medicine, Hokkaido University Graduate School of Medicine, Sapporo, Japan; [5]Gastroenterology and Hepatology, Musashino Red Cross Hospital, Tokyo, Japan; [6]Department of Internal Medicine, Hyogo College of Medicine, Nishinomiya, Japan; [7]Pathology, School of Medicine, Keio University, Japan; [8]Department of Pathology, Kurume University School of Medicine, Japan.

Received February 6, 2012; accepted April 22, 2012.

Supported by a grant (22-108) from the National Center for Global Health and Medicine in Japan and a grant from New Energy and Industrial Technology Development Organization of Japan.

reported using this method, leading to misdiagnosis of cirrhosis.[8] Therefore, finding a noninvasive method for diagnosing liver fibrosis is an emerging issue in the care of patients with CHC.

Several methods have been studied for the noninvasive diagnosis of hepatic fibrosis or cirrhosis, including clinical[9] or blood markers,[10,11] and signal analysis (ultrasonography, magnetic resonance imaging, and elastography).[12,13] Although each method can play a substantial role in the diagnosis of cirrhosis, it is evident that the best way of monitoring hepatitis progression employs an accurate serological method for the quantitative evaluation of fibrosis. We developed a new glyco-marker using multiple lectins that performed well in estimating liver fibrosis in a single-center study.[14,15]

Recent progress in glycoproteomics has had a great influence on work toward ideal, disease-specific biomarkers for a number of conditions. Glycoproteins that exhibit disease-associated glyco-alteration and are present in serum or other fluids have the potential to act as biomarkers for the diagnosis of a target disease,[16] because the features of glycosylation depend on the extent of cell differentiation and the stage of the cell. Detecting hepatic disease-associated glyco-markers for clinical applications has been a continuous challenge since the early 1990s, because increased fucosylation on complex-type *N*-glycans has been frequently detected in glycoproteins from patients with hepatocellular carcinoma (HCC) and cirrhosis.[17,18] Of all the alpha-fetoprotein (AFP) glycoforms, more than 30% have been found to react to a fucose-binding lectin, *Lens culinaris* agglutinin. This fraction, designated AFP-L3, was approved by the U.S. Food and Drug Administration (FDA) in 2005 for the diagnosis and prognosis of HCC.[19] We have found that two fibrosis-indicator lectins (*Aspergillus oryzae* lectin [AOL] and *Maackia amurensis* lectin [MAL]) together with an internal, standard lectin (*Datura stramonium* lectin [DSA]) on an alpha 1-acid glycoprotein (AGP) could, using lectin microarray, clearly distinguish between cirrhosis and chronic hepatitis patients.[14] We have further simplified this quantitative method so that it could be performed using bedside, clinical chemistry analyzers.[15]

The aim of the current study was to evaluate this new glyco-marker (LecT-Hepa) using multiple lectins and bedside clinical chemistry analyzers for use in the assessment of liver fibrosis. In this multicenter study we compared the method's efficiency in estimating liver fibrosis with other noninvasive fibrosis markers and tests.

Materials and Methods

Study Population. This study included 183 consecutive adult patients with CHC who had undergone percutaneous liver biopsy at one of the following institutions: Hokkaido University Hospital, Musashino Red Cross Hospital, National Center for Global Health and Medicine, Hyogo College of Medicine Hospital, or Nagoya City University Hospital in Japan. A diagnosis of CHC was defined as detectable serum anti-hepatitis C virus (HCV) antibody and HCV-RNA, found using polymerase chain reaction assays, of at least 2 points. Exclusion criteria were coinfection with hepatitis B virus or human immunodeficiency virus (HIV), and other disorders that commonly cause liver diseases. Informed consent was obtained from each patient who participated in the study. This study was conducted in accordance with the provisions of the Declaration of Helsinki and was approved by our Institutional Review Board.

Histological Staging. Ultrasonography-guided liver biopsy was performed according to a standardized protocol. Specimens were fixed, paraffin-embedded, and stained with hematoxylin-eosin and Masson's trichrome. A minimum of six portal tracts in the specimen were required for diagnosis. All liver biopsy samples were independently evaluated by two senior pathologists who were blinded to the clinical data. Liver fibrosis stages were assessed using METAVIR fibrosis (F) staging.[20] Significant fibrosis was defined as METAVIR F $\geq$2, severe fibrosis as METAVIR F $\geq$3, and cirrhosis as METAVIR F4. Two patients were excluded from the study because of inadequate histological samples.

Clinical and Biological Data. The age and sex of the patients were recorded. Serum samples were collected immediately before or no more than 2 months

Address reprint requests to: Masashi Mizokami, M.D., Ph.D., Research Center for Hepatitis and Immunology, National Center for Global Health and Medicine, 1-7-1, Konodai, Ichikawa 272-8516, Japan. E-mail: mmizokami@hospk.ncgm.go.jp; fax: +81-(0)47-375-4766.

View this article online at wileyonlinelibrary.com.

DOI 10.1002/hep.25815

Potential conflict of interest: Nothing to report.

after liver biopsy and were stored at −80°C until analysis. The concentrations of the following variables were obtained by analyzing the serum samples: aspartate aminotransferase (AST), alanine aminotransferase (ALT), gamma-glutamyltransferase (GGT), total bilirubin, albumin, cholinesterase, total cholesterol, platelet count (platelets), prothrombin time, haptoglobin, hyaluronic acid (HA), α2-macroglobulin (α2-MG), tissue inhibitors of metalloproteinases 1 (TIMP1). The aspartate aminotransferase-to-platelet ratio index (APRI), Fib-4 index, Forns index, and Zeng's score were calculated according to published formulae appropriate to each measure.[2,7,21,22]

Rapid Lectin-Antibody Sandwich Immunoassay Using HISCL. Fibrosis-specific glyco-alteration of AGP was qualified from simultaneous measurements of the lectin-antibody sandwich immunoassays using three lectins (DSA, MAL, and AOL). In principle, the glycan part of the AGP was captured by the lectin immobilized on the magnetic beads, and the captured AGP was then quantified by an antihuman AGP mouse monoclonal antibody probe that was cross-linked to an alkaline phosphatase (ALP-αAGP). The assay manipulation was fully automated using a chemiluminescence enzyme immunoassay machine (HISCL-2000i; Sysmex, Kobe, Japan). We used the following criterion formula, named the "LecT-Hepa Test," to enhance the diagnostic accuracy by combining two glyco-parameters (AOL/DSA and MAL/DSA) as described before: $F = \mathrm{Log}_{10}[\mathrm{AOL/DSA}]*8.6-[\mathrm{MAL/DSA}]$.[15]

Statistical Analyses. Quantitative variables were expressed as the mean ± standard deviation (SD) unless otherwise specified. Categorical variables were compared using a chi-squared test or Fisher's exact test, as appropriate, and continuous variables were compared using the Mann-Whitney U test. $P < 0.05$ was considered statistically significant. A multivariate forward stepwise logistic regression analysis was performed to determine the independent predictors of the absence or presence of significant fibrosis, severe fibrosis, and cirrhosis, respectively. Pearson's correlation coefficient was used as necessary. To assess the classification efficiencies of various markers for detecting significant fibrosis, severe fibrosis, and cirrhosis,[23] and to determine area under the curve (AUC) values, receiver-operating characteristic (ROC) curve analysis was also carried out. Diagnostic accuracy was expressed as the diagnostic specificity (specificity), diagnostic sensitivity (sensitivity), positive predictive values (PPV), negative predictive values (NPV), positive likelihood ratio (LR [+]), negative likelihood ratio (LR [−]), and AUC (95% confidence interval [95% CI]). We performed statistical analyses using STATA v. 11.0 (StataCorp, College Station, TX).

Table 1. Baseline Characteristics of the 183 Patients with Chronic Hepatitis C at the Time of Liver Biopsy

Features	Total (n = 183)
Age (years)	57.6 ± 11.4
Male sex	75 (41.0)
AST (IU/L)	57.4 ± 43.9
ALT (IU/L)	62.8 ± 56.8
GGT (IU/L)	51.1 ± 62.6
Bilirubin (mg/dL)	0.7 ± 0.4
Albumin (g/L)	4.1 ± 0.4
Cholinesterase (IU/L)	283.5 ± 97.0
Cholesterol (mg/dL)	174.1 ± 35.5
Platelets (10^9/L)	163 ± 57
Prothrombin time (%)	87.2 ± 33.4
α2-MG (g/L)	356.8 ± 133.1
HA (μg/L)	205.3 ± 428.0
TIMP1 (pg/ml)	210.6 ± 87.7
AOL/DSA	6.3 ± 12.3
MAL/DSA	9.0 ± 3.1
Fibrosis stage (%):	
F0-1	89 (48.6)
F2	46 (25.1)
F3	22 (12.0)
F4	26 (14.2)

Results

Baseline Characteristics of the 183 Patients with Chronic Hepatitis C at the Time of Liver Biopsy. Patient characteristics at the time of liver biopsy are shown in Table 1. The mean age of the 183 patients was 57.6 ± 11.4 years, and 75 (41%) of them were men. F0-F1 was diagnosed in 89 cases (48.6%), F2 in 46 (25.1%), F3 in 22 (12.0%), and F4 (cirrhosis) in 26 (14.2%).

Comparison of Variables Associated with the Presence of Significant Fibrosis by Univariate and Multivariate Analysis. Variables associated with the presence of significant fibrosis were assessed by univariate and multivariate analysis (Table 2). The variables of age ($P = 0.001$), AST ($P < 0.0001$), ALT ($P < 0.0001$), GGT ($P < 0.0001$), bilirubin ($P = 0.014$), α2-MG ($P = 0.002$), HA ($P < 0.0001$), TIMP1 ($P < 0.0001$), and AOL/DSA ($P < 0.0001$) were significantly higher in the significant fibrosis group than in the not significant fibrosis group. The variables albumin ($P < 0.001$), cholinesterase ($P < 0.0001$), cholesterol ($P = 0.005$), platelets ($P < 0.0001$), prothrombin time ($P = 0.0001$), and MAL/DSA ($P < 0.0001$) were significantly lower in the significant fibrosis group than in the not significant fibrosis group. Multivariate analysis showed that platelets (odds ratio [OR]: 0.87,

Table 2. Variables Associated with the Presence of Significant Fibrosis (F2-4) and Severe Fibrosis (F3-4) by Univariate and Multivariate Analysis

Features	No Significant Fibrosis (n = 89)	Significant Fibrosis (n = 94)	P Value (Univariate)	Odds Ratio (95% CI) (Multivariate)	No Severe Fibrosis (n = 135)	Severe Fibrosis (n = 48)	P Value	Odds Ratio (95% CI) (Multivariate)
Age (years)	54.7 ± 11.8	60.5 ± 10.4	0.001		55.8 ± 11.9	62.9 ± 7.8	0.001	1.15 (1.02-1.31)
Male sex (%)	30 (33.7)	45 (47.9)	0.051		52 (38.5)	23 (47.9)	0.255	
AST (IU/L)	45.7 ± 41.6	68.3 ± 43.5	<0.0001		49.7 ± 40.1	79.1 ± 47.4	<0.0001	
ALT (IU/L)	51.0 ± 56.6	74.0 ± 54.9	<0.0001		55.9 ± 54.9	82.5 ± 57.9	<0.0001	
GGT (IU/L)	40.6 ± 61.7	62.1 ± 63.1	<0.0001		45.5 ± 67.1	65.8 ± 46.7	<0.0001	
Bilirubin (mg/dL)	0.6 ± 0.3	0.7 ± 0.4	0.014		0.6 ± 0.3	0.8 ± 0.4	0.005	
Albumin (g/L)	4.2 ± 0.3	4.0 ± 0.5	<0.001		4.2 ± 0.3	3.8 ± 0.5	<0.0001	
Cholinesterase (IU/L)	329.2 ± 76.0	247.2 ± 96.9	<0.0001		312.4 ± 84.4	217 ± 91.9	<0.0001	
Cholesterol (mg/dL)	181.0 ± 31.5	167.5 ± 36.2	0.005		178.1 ± 34.1	162.4 ± 33.5	0.016	
Platelets (10^9/L)	186 ± 53	142 ± 52	<0.0001	0.87 (0.77-0.99)	180 ± 52	119 ± 46	<0.0001	0.74 (0.58-0.94)
Prothrombin time (%)	94.7 ± 33.4	80.1 ± 32.1	0.0001		89.5 ± 36.2	80.8 ± 23.2	<0.001	
α2-MG (g/L)	326 ± 117.7	389.2 ± 141.1	0.002		331.1 ± 122.5	423.9 ± 137.5	<0.0001	
HA (μg/L)	85.6 ± 154.3	318.7 ± 556.1	<0.0001	1.01 (1.01-1.02)	115.4 ± 201.1	458.2 ± 711.0	<0.0001	
TIMP1 (pg/ml)	183.5 ± 53.3	238.6 ± 106.1	<0.0001		189.7 ± 64.5	263.9 ± 113.8	<0.0001	
AOL/DSA	1.4 ± 1.2	10.9 ± 15.9	<0.0001	1.51 (1.07-2.15)	2.0 ± 2.6	18.3 ± 19.3	<0.0001	
MAL/DSA	10.6 ± 1.7	7.5 ± 3.4	<0.0001		10.2 ± 2.0	5.6 ± 3.4	<0.0001	0.52 (0.37-0.76)

95% CI: 0.77-0.99), HA (OR: 1.01, 95% CI: 1.01-1.02), and AOL/DSA (OR: 1.51, 95% CI: 1.07-2.15) were independently associated with the presence of significant fibrosis.

Comparison of Variables Associated with the Presence of Severe Fibrosis by Univariate and Multivariate Analysis. Variables associated with the presence of severe fibrosis were assessed by univariate and multivariate analysis (Table 2). The variables of age ($P = 0.001$), AST ($P < 0.0001$), ALT ($P < 0.0001$), GGT ($P < 0.0001$), bilirubin ($P = 0.005$), α2-MG ($P < 0.0001$), HA ($P < 0.0001$), TIMP1 ($P < 0.0001$), and AOL/DSA ($P < 0.0001$) were significantly higher in the severe fibrosis group than in the no severe fibrosis group. The variables albumin ($P < 0.0001$), cholinesterase ($P < 0.0001$), cholesterol ($P = 0.016$), platelets ($P < 0.0001$), prothrombin time ($P < 0.001$), and MAL/DSA ($P < 0.0001$) were significantly lower in the severe fibrosis group than in the no severe fibrosis group. Multivariate analysis showed that age (OR: 1.15, 95% CI: 1.02-1.31), platelets (OR: 0.74, 95% CI: 0.58-0.94), and MAL/DSA (OR: 0.52, 95% CI:

Table 3. Variables Associated with the Presence of Cirrhosis (F4) by Univariate and Multivariate Analysis

Features	No Cirrhosis (n=157)	Cirrhosis (n = 26)	P Value	Odds Ratio (95% CI) (Multivariate)
Age (years)	56.6 ± 11.7	63.8 ± 7.3	0.0016	
Male sex (%)	60 (38.2)	15 (57.7)	0.061	
AST (IU/L)	54.6 ± 41.7	74.9 ± 53.7	0.016	
ALT (IU/L)	62.1 ± 58.1	67.2 ± 48.2	0.446	
GGT (IU/L)	48.5 ± 63.9	64.9 ± 53.8	0.0031	
Bilirubin (mg/dL)	0.6 ± 0.3	1.0 ± 0.5	<0.0001	
Albumin (g/L)	4.2 ± 0.4	3.6 ± 0.5	<0.0001	
Cholinesterase (IU/L)	305.3 ± 83.9	181.7 ± 90.1	<0.0001	
Cholesterol (mg/dL)	178.4 ± 33.3	146.9 ± 29.8	<0.0001	
Platelets (10^9/L)	172 ± 54	106 ± 36	<0.0001	0.76 (0.58-0.99)
Prothrombin time (%)	88.7 ± 35.5	79.2 ± 16.1	0.0004	
α2-MG (g/L)	346.2 ± 131.6	416.9 ± 127.8	0.019	
HA (μg/L)	137.1 ± 215.7	617.4 ± 915.1	<0.0001	
TIMP1 (pg/ml)	196.4 ± 70.4	287.3 ± 126.6	<0.0001	
AOL/DSA	3.4 ± 7.1	24.0 ± 20.4	<0.0001	
MAL/DSA	9.8 ± 2.4	4.2 ± 2.8	<0.0001	0.67 (0.49-0.90)